

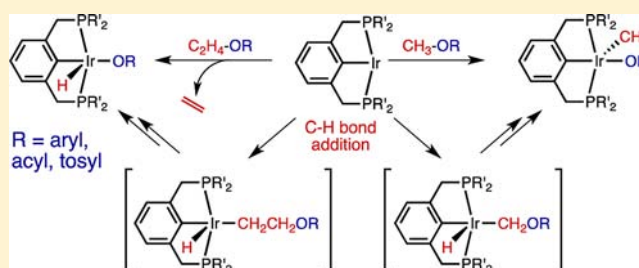
# Cleavage of Ether, Ester, and Tosylate C(sp<sup>3</sup>)–O Bonds by an Iridium Complex, Initiated by Oxidative Addition of C–H Bonds. Experimental and Computational Studies

Sabuj Kundu, Jongwook Choi, David Y. Wang, Yuriy Choliy, Thomas J. Emge, Karsten Krogh-Jespersen,\* and Alan S. Goldman\*

Department of Chemistry and Chemical Biology, Rutgers, The State University of New Jersey, New Brunswick, New Jersey 08903, United States

**S** Supporting Information

**ABSTRACT:** A pincer-ligated iridium complex, (PCP)Ir (PCP =  $\kappa^3$ -C<sub>6</sub>H<sub>3</sub>-2,6-[CH<sub>2</sub>P(*t*-Bu)<sub>2</sub>]<sub>2</sub>), is found to undergo oxidative addition of C(sp<sup>3</sup>)–O bonds of methyl esters (CH<sub>3</sub>–O<sub>2</sub>CR'), methyl tosylate (CH<sub>3</sub>–OTs), and certain electron-poor methyl aryl ethers (CH<sub>3</sub>–OAr). DFT calculations and mechanistic studies indicate that the reactions proceed via oxidative addition of C–H bonds followed by oxygenate migration, rather than by direct C–O addition. Thus, methyl aryl ethers react via addition of the methoxy C–H bond, followed by  $\alpha$ -aryloxide migration to give *cis*-(PCP)Ir(H)-(CH<sub>2</sub>)<sub>2</sub>(OAr), followed by iridium-to-methylidene hydride migration to give (PCP)Ir(CH<sub>3</sub>)(OAr). Methyl acetate undergoes C–H bond addition at the carbomethoxy group to give (PCP)Ir(H)[ $\kappa^2$ -CH<sub>2</sub>OC(O)Me] which then affords (PCP-CH<sub>2</sub>)Ir(H)( $\kappa^2$ -O<sub>2</sub>CMe) (**6-Me**) in which the methoxy C–O bond has been cleaved, and the methylene derived from the methoxy group has migrated into the PCP C<sub>ipso</sub>–Ir bond. Thermolysis of **6-Me** ultimately gives (PCP)Ir(CH<sub>3</sub>)( $\kappa^2$ -O<sub>2</sub>CR), the net product of methoxy group C–O oxidative addition. Reaction of (PCP)Ir with species of the type ROAr, RO<sub>2</sub>CMe or ROTs, where R possesses  $\beta$ -C–H bonds (e.g., R = ethyl or isopropyl), results in formation of (PCP)Ir(H)(OAr), (PCP)Ir(H)(O<sub>2</sub>CMe), or (PCP)Ir(H)(OTs), respectively, along with the corresponding olefin or (PCP)Ir(olefin) complex. Like the C–O bond oxidative additions, these reactions also proceed via initial activation of a C–H bond; in this case, C–H addition at the  $\beta$ -position is followed by  $\beta$ -migration of the aryloxide, carboxylate, or tosylate group. Calculations indicate that the  $\beta$ -migration of the carboxylate group proceeds via an unusual six-membered cyclic transition state in which the alkoxy C–O bond is cleaved with no direct participation by the iridium center.



## 1. INTRODUCTION

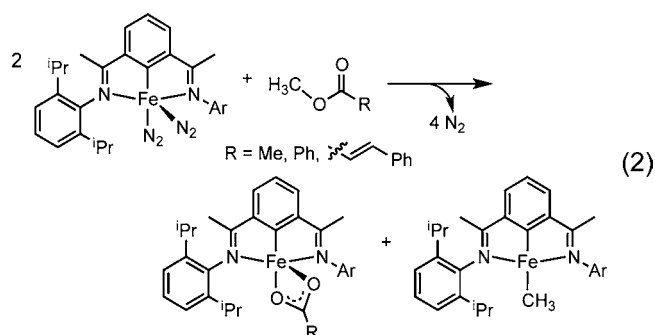
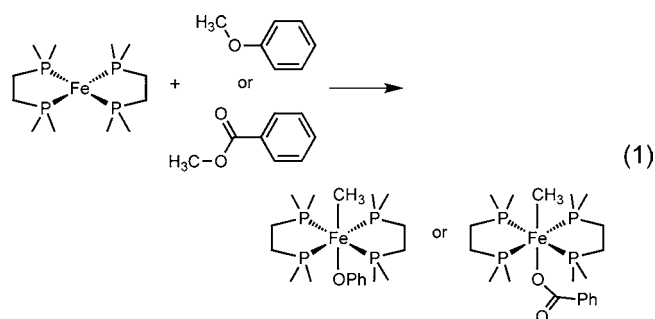
Carbon–oxygen bonds are ubiquitous in nature and are among the most fundamental linkages in organic chemistry. Accordingly, transformations of C–O bonds to other functional groups and the removal of oxygen-containing groups rank among the most attractive challenges in modern catalysis. Increasing interest in the conversion of biomass to fuel as an alternative to petroleum-based feedstocks has spurred research in C–O bond activation as this will require removal of oxygen from the “overfunctionalized” biomass.<sup>1–10</sup> Alternatively, partial deoxygenation of biomass could lead to higher value chemical products. Recent progress in transition-metal catalyzed C–C or C–X bond coupling reactions, achieved by activating sp<sup>2</sup> or benzylic-type sp<sup>3</sup> C–O bonds in ethers<sup>11–23</sup> and esters<sup>24–32</sup> has also elevated interest in C–O bond activation. However, while numerous studies have been reported involving cleavage of activated C–O bonds such as those in allyl esters or ethers,<sup>33–36</sup> the catalytic activation of sp<sup>3</sup> C–O bonds has been relatively unexplored and remains a significant challenge.

Oxidative addition is one of the most fundamental processes in organometallic chemistry and is a key step in many transformations catalyzed by transition-metal complexes. The oxidative addition of carbon–halogen and carbon–hydrogen bonds has been and continues to be extensively studied.<sup>37–40</sup> In a seminal study in 1978, Ittel and Tolman showed that the Fe(0) intermediate Fe(dmpe)<sub>2</sub> (dmpe = Me<sub>2</sub>PCH<sub>2</sub>CH<sub>2</sub>PMe<sub>2</sub>) undergoes oxidative addition reactions with anisole or methyl benzoate, affording Fe(dmpe)<sub>2</sub>(CH<sub>3</sub>)(OPh) or Fe(dmpe)<sub>2</sub>(CH<sub>3</sub>)(O<sub>2</sub>CPh), respectively (eq 1).<sup>41,42</sup> Since then, however, although several examples have been reported of oxidative addition with cyclic ethers or sp<sup>2</sup> C–O bonds,<sup>15,43–48</sup> reports of oxidative addition of sp<sup>3</sup> C–O bonds in ethers and esters have been extremely limited.<sup>49</sup>

In 2008, Chirik et al. reported that (<sup>i</sup>PrPDI)Fe(N<sub>2</sub>)<sub>2</sub> cleaves the C–O bonds in alkyl-substituted esters via a binuclear oxidative addition (eq 2).<sup>47</sup> Other notable examples of

Received: December 31, 2012

Published: March 7, 2013



unactivated  $sp^3$  C–O bond cleavage include Carmona and Paneque's seminal discovery of the rearrangement reactions of methyl aryl ethers by a tris(pyrazolyl)borate iridium complex,<sup>50</sup> reports by Ozerov and Grubbs of cleavage of the *tert*-butyl-oxygen and benzyl-oxygen bonds of methyl ethers by a PNP-pincer Ir complex,<sup>51,52</sup> and Jones' report of the cleavage of the methoxy C–O bond of methyl-acetate by a diphosphine platinum complex.<sup>32</sup>

The pincer-ligated complex (PCP)Ir (PCP =  $\kappa^3$ -C<sub>6</sub>H<sub>3</sub>-2,6-[CH<sub>2</sub>P(*t*-Bu)<sub>2</sub>]<sub>2</sub>) and its derivatives are the most efficient alkane dehydrogenation catalysts developed to date.<sup>53–55</sup> This species also activates  $sp^2$  C–H bonds of arenes or vinyl moieties,<sup>56</sup> C–X (X = halogen) bonds,<sup>57</sup> O–H bonds of water and alcohols,<sup>58,59</sup> and the N–H bond of aniline.<sup>60</sup> Recently, we reported the oxidative addition of C( $sp^3$ )–F bonds by (PCP)Ir.<sup>61</sup>

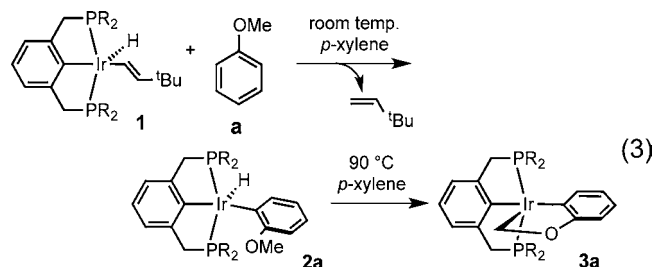
As part of our efforts to activate unreactive bonds in small molecules, we have investigated C–O bond cleavage by (PCP)Ir. Herein, we report that reactions of (PCP)Ir with alkyl esters, certain electron-poor alkyl aryl ethers, and alkyl tosylates result in oxidative addition or other cleavage reactions of the C( $sp^3$ )–O bond. Results from DFT calculations as well as experimental evidence indicate that C–O bond cleavage in these substrates proceeds via initial activation of a C–H bond, rather than direct C–O insertion or nucleophilic attack. These mechanistic findings have obvious implications for the microscopically reverse C–O bond formation reactions.<sup>62,63</sup> Parts of this study have been previously communicated.<sup>64</sup>

## 2. RESULTS AND DISCUSSION

### 2.1. Reactions of (PCP)Ir with Methyl Oxygenates MeOAr, MeOTs, MeOAc, and MeO<sub>2</sub>CPh. 2.1.1. Reaction of (PCP)Ir with Methyl Aryl Ethers.

The reactive 14e<sup>−</sup> three-coordinate species (PCP)Ir may be generated by loss of olefin from (PCP)Ir(TBV)(H) (**1**, TBV = 3,3-dimethyl-1-butenyl) or (PCP)Ir(NBE) (**1'**, NBE = 2-norbornene), as previously reported;<sup>60,65,66</sup> these two approaches have been used interchangeably in this study.

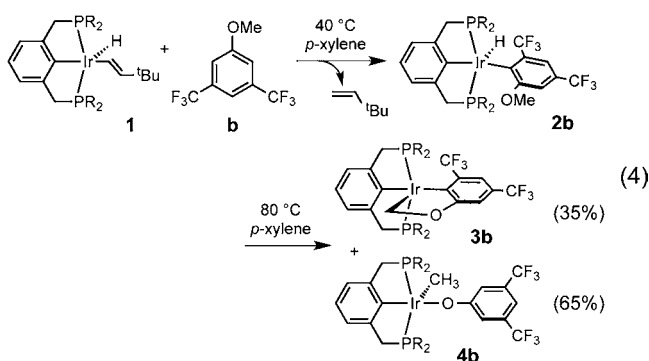
In an initial experiment in this study, the reaction of (PCP)Ir with anisole, the simplest methyl aryl ether, was investigated. Treatment of **1** or **1'** with anisole (**a**; 1.05 equiv) in *p*-xylene-*d*<sub>10</sub> at room temperature resulted in an immediate color change from dark red to red (eq 3; PR<sub>2</sub> = P<sup>*t*</sup>Bu<sub>2</sub> for all structures



shown). Selectively proton-decoupled <sup>31</sup>P NMR spectroscopy revealed one major signal, a doublet at 68.2 ppm ( $J_{HP} = 12.2$  Hz). A hydride resonance in the <sup>1</sup>H NMR spectrum appears as a sharp triplet ( $J_{HP} = 14.4$  Hz) at −45.03 ppm, characteristic of a square pyramidal five-coordinate complex in which the hydride occupies the axial site.<sup>67</sup> These signals were assigned to the C–H addition product **2a**. The hydride resonance is sharp at room temperature, in contrast with the previously reported aryl hydride complex (PCP)Ir(Ph)(H) in which the hydride signal is sharp only at or below ca. −40 °C, due to rapid reversible reductive elimination of benzene.<sup>56</sup> DFT calculations (see Supporting Information, SI, for details) indicate that C–H bond addition to give complex **2a** is 3.7 kcal/mol more exergonic than benzene C–H addition, presumably at least in part because of a weak favorable interaction between the methoxy group and the iridium center in **2a** (computed Ir–O distance = 3.02 Å).

Heating the reaction mixture for 3 h at 90 °C results in the formation of cyclometalated product (PCP)Ir( $\kappa^2$ -CH<sub>2</sub>OC<sub>6</sub>H<sub>4</sub>) (**3a**) in quantitative yield (eq 3). Characterization of **3a** by NMR spectroscopy and X-ray crystallography has been reported,<sup>64</sup> and analogous cyclometalated adducts have been reported previously by Wilkinson,<sup>68</sup> Carmona,<sup>67,69,70</sup> and Perutz and co-workers.<sup>71</sup> DFT calculations indicate that the key step in the reaction of **2a** to afford **3a** (and H<sub>2</sub>), cleavage of the methoxy C–H bond, proceeds via an Ir(V) intermediate which readily loses H<sub>2</sub>. The reaction is calculated to be endergonic ( $\Delta G_{rx} = 7.0$  kcal/mol at  $P = 1$  atm,  $T = 25$  °C), but presumably the released dihydrogen is readily scavenged by the excess olefinic hydrogen acceptor present under the reaction conditions.

In an effort to prevent formation of products like **2a** and **3a**, and thereby allow the formation of C–O addition products instead, we investigated the reaction of **1** with 2,6-dimethyl anisole and 3,5-dimethyl anisole (in which the ortho C–H bonds are substituted or sterically hindered, respectively). Heating the reaction mixture at 100 °C, however, only produced a complex mixture of unidentified products. In order to favor C–O addition, we then turned to electron-withdrawing trifluoromethyl groups to block the ortho C–H bonds. Despite the steric bulk of such groups, however, when **1** equiv. of (PCP)Ir(TBV)(H) (**1**) was treated with 3,5-bis(trifluoromethyl)anisole (**b**) in *p*-xylene at 40 °C, the ortho C–H activation product **2b** formed cleanly (eq 4; see SI for NMR spectroscopic characterization). Apparently, although the presence of an ortho methyl group strongly disfavors addition to (PCP)Ir,<sup>56</sup> the even greater steric effects of the



trifluoromethyl group are more than compensated for by its favorable electronic effects.<sup>71–75</sup>

In view of the known reversibility of aryl C–H activation by (PCP)Ir,<sup>56</sup> we subjected complex **2b** to thermolysis; to our gratification, after 5 h at 80 °C the formation of (PCP)Ir(CH<sub>3</sub>)(3,5-bis(trifluoromethyl)phenoxy) (**4b**) was observed in 65% yield, along with complex **3b** in 35% yield (eq 4).<sup>64</sup> Both **3b** and **4b** were characterized by NMR spectroscopy, and the structure of **4b** was confirmed by X-ray crystallography.<sup>64</sup> To our knowledge, complex **4b** is only the second reported example of intermolecular oxidative addition to a transition metal of an alkyl carbon–oxygen bond in simple ethers (the first example being that in eq 1).<sup>41,42</sup>

The formation of cyclometalated product **3b** led us to investigate the use of substrates in which ortho C–H bond activation is fully prevented, while the electron-poor character of the aryl ring is maintained or increased. When **1** was treated with 1.05 equiv. of pentafluoroanisole (**c**) at room temperature, an immediate color change from dark red to red was observed.

NMR spectroscopy as well as X-ray crystallography revealed the quantitative formation of (PCP)Ir(CH<sub>3</sub>)(OC<sub>6</sub>F<sub>5</sub>) (**4c**) resulting from oxidative addition of the C(sp<sup>3</sup>)–O bond;<sup>64</sup> no side-products or intermediates were observed during the reaction process. 4-methoxy-2,3,5,6-tetrafluorotoluene (**d**) likewise reacted with **1** immediately at room temperature and analogously afforded (PCP)Ir(CH<sub>3</sub>)(2,3,5,6-tetrafluoro-4-methyl phenoxy) (**4d**) in quantitative yield.<sup>64</sup>

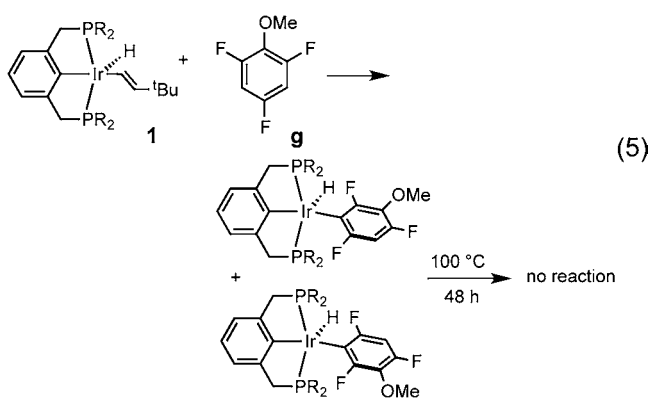
To probe the scope of the C–O addition, reactivity with various other fluorine-substituted methyl aryl ethers was investigated; results are summarized in Table 1. All reactions were carried out at 100 °C in *p*-xylene solution, except reactions of arenes **c** and **d** which were conducted at room temperature. Arenes **e** and **f**, also fluorinated ortho to the methoxy group, gave C–O oxidative adducts (**4**) as the major products although yields were lower than obtained with the more highly fluorinated arenes **c** and **d**. In the case of 2,4,6-trifluoroanisole (**g**), two rotamers of the aryl C–H adduct, (PCP)Ir(H)(2,4,6-trifluoro-3-methoxyphenoxy), were the only products obtained, even after heating for two days at 100 °C (eq 5); no C–O oxidative addition product, viz. (PCP)Ir(CH<sub>3</sub>)(2,4,6-trifluorophenoxy), was observed. This result is consistent with the favorable effect of ortho-F substituents (of which there are two in this case) on the stability of metal aryl complexes as demonstrated by Perutz, Jones, Eisenstein, and co-workers.<sup>71–75</sup>

The presence of C–H bonds ortho to the methoxy group (substrates **h**, **i**, and **j**) resulted in complete conversion to cyclometalated C–H addition products analogous to complex **3a**, which was formed in the case of anisole. The structures of complexes **3h** and **3j** were confirmed by X-ray crystallography (see Figures S1 and S2 of the SI). The stability of these

**Table 1. Oxidative Addition of the C–O Bond in Various Fluorine-Substituted Methyl Aryl Ethers<sup>a</sup>**

Substrate	Yield		Substrate	Yield	
	<b>3</b>	<b>4</b>		<b>3</b>	<b>4</b>
(c) <sup>b</sup> 	0	> 99 %	(g) 	0	0
(d) <sup>b</sup> 	0	> 99 %	(h) 	> 99 %	0
(e) 	0	70 %	(i) <sup>c</sup> 	> 99 %	0
(f) 	0	65 %	(j) 	> 99 %	0

<sup>a</sup>General reaction conditions: (PCP)Ir(TBV)(H) (20–25 μmol) + 1.05 equiv. of substrate in *p*-xylene solution at 100 °C for 15–20 h. <sup>b</sup>Room temperature. <sup>c</sup>30 h.

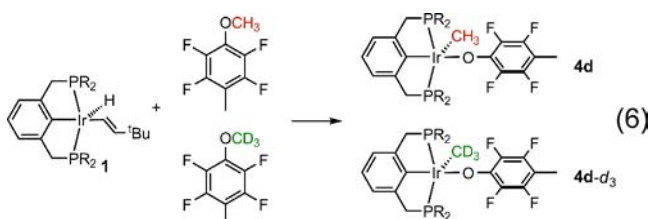


derivatives of **3** is presumably increased by the fluorine substitution of the ring.<sup>71–75</sup>

**2.1.2. Mechanism of Ether C–O Bond Addition.** As noted above, reports of oxidative addition of ether C(sp<sup>3</sup>)–O bonds are limited, the only previous intermolecular example being the Ittel-Tolman system (eq 1). In that case, the reaction probably proceeds via an S<sub>N</sub>2-type nucleophilic attack by the very electron-rich Fe(0) center on the electrophilic anisole methyl group, thus accounting for formation of the trans addition product.<sup>28,29</sup> Milstein and co-workers proposed two different activation mechanisms for C–O bond cleavage in aryl methyl ether pincer precursors by Rh, Pd, and Ni complexes.<sup>45,46</sup> They suggested that electron-rich, nucleophilic Rh complexes cleave sp<sup>3</sup> C–O bonds via a concerted, three-centered transition state (direct C–O addition), whereas electron-deficient Pd or Ni complexes were proposed to cleave sp<sup>3</sup> C–O bonds via electrophilic interaction with the oxygen atom.

For the current set of reactions, nucleophilic attack did not a priori seem likely as (PCP)Ir is not expected to be a strong nucleophile. Rather, the reactivity of (PCP)Ir is dominated by the vacant coordination site trans to the aryl group (essentially an empty site in a d<sup>8</sup> square planar configuration), with some contribution from the filled d-orbitals of π-symmetry. The most obvious mechanism consistent with this electronic configuration would be the direct, concerted, insertion of Ir into the C–O bond. However, in view of the proclivity of (PCP)Ir toward addition of C–H bonds, we investigated the effect of isotopic substitution of the methoxy hydrogen atoms.

A mixture of 4-methoxy-2,3,5,6-tetrafluorotoluene and its deuterated methoxy analogue (at least 7 fold excess of each substrate) was added to a *p*-xylene solution of **1**. An immediate color change from dark red to red was observed and two resonances due to (PCP)Ir(CH<sub>3</sub>)(2,3,5,6-tetrafluoro-4-methylphenoxide) (**4d**) and (PCP)Ir(CD<sub>3</sub>)(2,3,5,6-tetrafluoro-4-methylphenoxide) (**4d-d<sub>3</sub>**), respectively, appeared in the <sup>31</sup>P NMR spectrum at δ 47.26 and 47.48 ppm (eq 6). The product ratio of **4d** to **4d-d<sub>3</sub>** was determined by integration of the two <sup>31</sup>P NMR resonances and by integration of the Ir–CH<sub>3</sub> and the IrOC<sub>6</sub>F<sub>4</sub>CH<sub>3</sub> signals in the <sup>1</sup>H NMR spectrum.



A kinetic isotope effect,  $KIE_{\text{obs}} = k_{\text{ArOCH}_3}/k_{\text{ArOCD}_3} = 4.3(3)$  for the overall reaction **6**, was determined at room temperature from the product distribution as an average of three independent experiments. We note that this experiment reflects information regarding only the nature of the transition state for the critical product-determining step,<sup>76</sup> specifically only the relative energies of the two isotopomeric TSs (relative to the free ethers). In particular, it may be noted that the observed KIE is independent of whether or not (PCP)Ir and ether are complexed in the lowest energy (resting) state. This point is illustrated in Scheme 1, which indicates that the relative rates of reaction of CH<sub>3</sub>OAr and CD<sub>3</sub>OAr will depend (as per the Curtin-Hammett principle) only on  $\Delta\Delta G^\ddagger$  (eq 7); because of the nature of a competition experiment,  $\Delta G^\ddagger$  for formation of either isotopomer relates to the same resting state (or states).

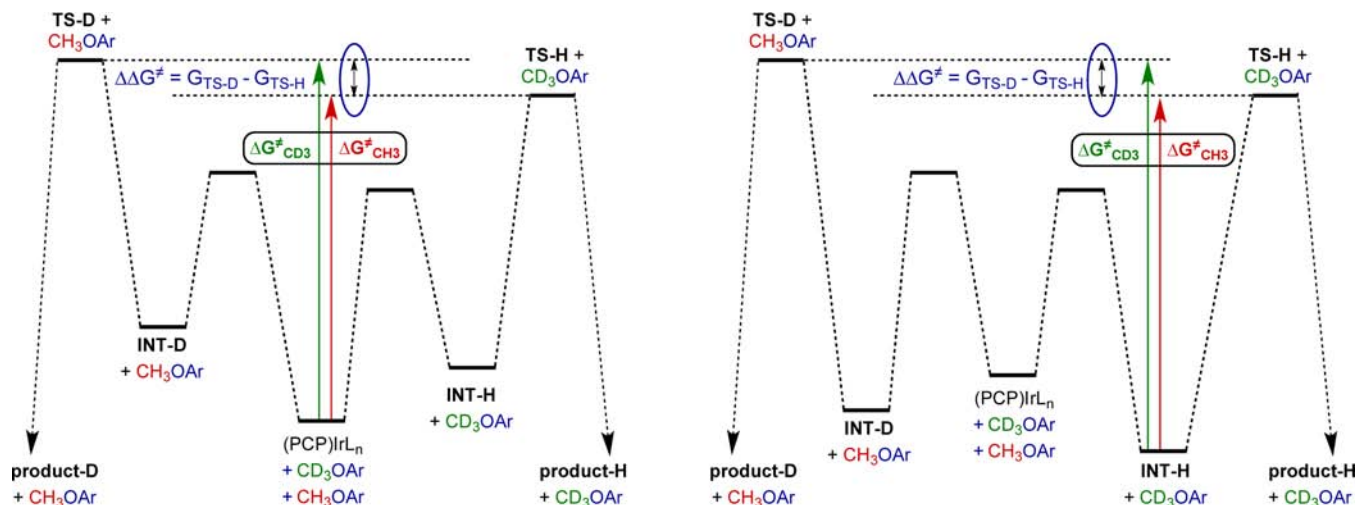
$$\Delta G_{\text{CX}_3}^\ddagger = G_{\text{TS-X}} - G_{\text{RS}} \quad (\text{X = H or D}) \quad (7a)$$

$$\begin{aligned} \Delta\Delta G^\ddagger &= (G_{\text{TS-D}} - G_{\text{RS}}) - (G_{\text{TS-H}} - G_{\text{RS}}) \\ &= G_{\text{TS-D}} - G_{\text{TS-H}} \end{aligned} \quad (7b)$$

The high observed kinetic isotope effect,  $k_{\text{ArOCH}_3}/k_{\text{ArOCD}_3} = 4.3(3)$ , is inconsistent with either a direct C–O addition or an S<sub>N</sub>2-type mechanism.<sup>77,78</sup> Instead, it implies that the rate-determining transition state features one or more C–H bonds that have been cleaved or at least significantly weakened. The high KIE<sub>obs</sub> indicates, particularly in view of the propensity of (PCP)Ir to undergo oxidative addition of C–H bonds, that the C–O addition proceeds, rather unexpectedly, via addition of a methoxy C–H bond. The simplest pathway to proceed from a C–H addition intermediate to the C–O addition product is that shown in Scheme 2.

DFT calculations (using M06 functionals, see Computational Methods) on the full (nontruncated) complexes were conducted for both the mechanism proposed in Scheme 2 and for a direct C–O addition mechanism. Using 4-MeO-*p*-C<sub>6</sub>F<sub>4</sub>Me as the substrate aryl ether (substrate **d**, Table 1), direct oxidative addition (3-centered transition state) of (PCP)Ir to the O–Me bond would encounter a barrier that is quite high ( $G_{\text{TS}} = 33.4$  kcal/mol relative to the ether and free three-coordinate (PCP)Ir). The reaction pathway proposed in Scheme 2 is calculated to be more favorable by almost 18 kcal/mol (Figure 1).

Initial activation of a methoxy group sp<sup>3</sup> C–H bond (transition state  $G_{\text{TS}} = 8.2$  kcal/mol; all values of  $G$  are given relative to free (PCP)Ir and the free organic species) yields a five-coordinate alkyl hydride intermediate ( $G = -4.5$  kcal/mol). The TS for  $\alpha$ -aryloxy elimination from this species is calculated to have a free energy  $G_{\text{TS}} = 14.6$  kcal/mol and leads to the methylene hydride aryloxy ( $G = 2.8$  kcal/mol). Subsequent 1,2-migration of hydride from Ir to the carbene ( $G_{\text{TS}} = 15.8$  kcal/mol) affords the observed product **4d** ( $G = -26.4$  kcal/mol). The difference in TS energies calculated for the 1,2-hydride migration (15.8 kcal/mol) and for  $\alpha$ -aryloxy elimination (14.6 kcal/mol) is small and probably not reliable considering the level of precision expected of the calculations when comparing species of a fairly different nature. Relative to the reactant (PCP)Ir(TBV)(H) (**1**) ( $G = -4.7$  kcal/mol), the calculated overall free energy activation barrier is thus 19–21 kcal/mol, which is consistent with a reaction that proceeds rapidly at room temperature (predicted half-life of approximately 10<sup>2</sup> s at 25 °C). In contrast, the calculated barrier for

Scheme 1. Hypothetical Free Energy Diagrams for the CH<sub>3</sub>OAr/CD<sub>3</sub>OAr Competition Reaction<sup>a</sup>

<sup>a</sup>In the diagram on the left, the implied resting state for iridium is not complexed with the ether (e.g., (PCP)Ir(TBV)(H)) while on the right, iridium and ether are associated in the resting state [e.g., (PCP)Ir(CH<sub>3</sub>OAr) or (PCP)Ir(H)(CH<sub>2</sub>OAr)]. In either case, the observed KIE will reflect only the energy difference between the isotopomeric TSs for the rate-determining step and the free ethers ( $\Delta\Delta G^\ddagger = G_{\text{TSD}} - G_{\text{TSH}}$ ).

## Scheme 2. Proposed Mechanism for Formation of 4 from 1 and Methyl Aryl Ethers

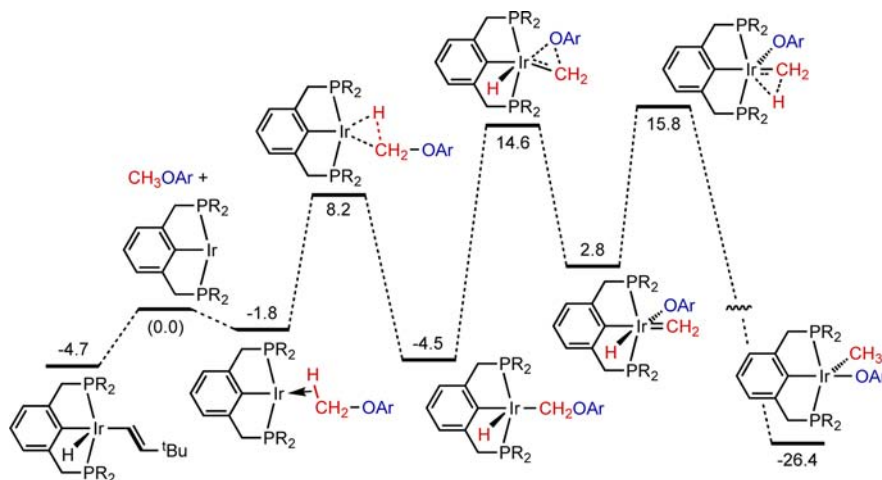
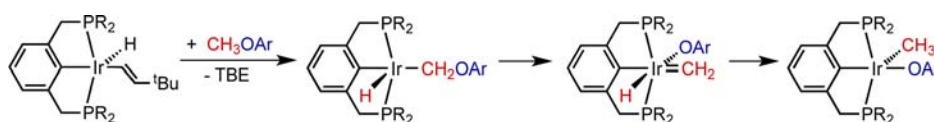


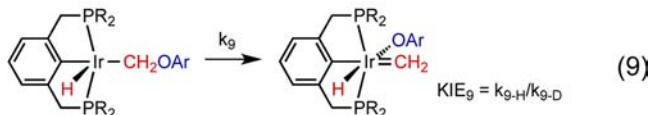
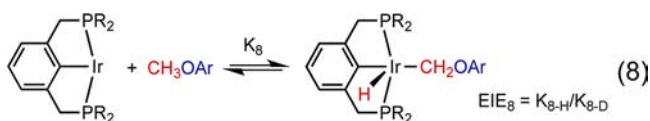
**Figure 1.** Calculated Gibbs free energies (kcal/mol) for reaction of (PCP)Ir and CH<sub>3</sub>-OAr, Ar = *p*-C<sub>6</sub>F<sub>4</sub>Me. Values of *G* are given relative to free (PCP)Ir and CH<sub>3</sub>-OAr. The free energies correspond to a reference state of 1 M concentration for each species participating in the reaction and *T* = 298.15 K. Potential energies, enthalpies, entropies and free energies for reaction of (PCP)Ir + CH<sub>3</sub>-OAr, Ar = *p*-C<sub>6</sub>F<sub>4</sub>Me are summarized in Table S1 of the SI.

direct C–O addition (relative to (PCP)Ir(TBV)(H)) is  $G^\ddagger = 38.1$  kcal/mol (corresponding to a half-life of ca.  $10^{15}$  s).

The free energies calculated for the 1,2-hydride migration and  $\alpha$ -aryloxy elimination TSs differ only by 1.2 kcal/mol (Figure 1). The computed KIEs, however, are significantly dependent on which TS effectively determines the rate, with  $k_{\text{ArOCH}_3}/k_{\text{ArOCD}_3}$  values of 4.24 or 7.23 predicted depending on whether  $\alpha$ -aryloxy elimination or 1,2-hydride migration is rate-determining. The former value is in excellent agreement with the experimentally determined  $\text{KIE}_{\text{obs}}$ ,  $k_{\text{OCH}_3}/k_{\text{OCD}_3} = 4.3(3)$ ; it therefore seems likely that  $\alpha$ -aryloxy migration is in fact rate-determining.<sup>79</sup> The overall reaction may thus be viewed as a

pre-equilibrium between (PCP)Ir (or its precursor, 1) and (PCP)Ir(CH<sub>2</sub>OAr)(H) (eq 8), followed by rate-determining 1,2-OAr migration (eq 9). Accordingly, the overall  $\text{KIE}_{\text{obs}}$  may be regarded as the product of the EIE for eq 8 and the KIE for eq 9.<sup>80</sup>

The EIE (at 25 °C) calculated for formation of the aryloxymethyl hydride ( $\text{EIE}_8 = K_{8\text{-H}}/K_{8\text{-D}}$ ) is 3.12 ( $\Delta\Delta G_8 = -0.674$  kcal/mol) while  $\text{KIE}_9$  ( $k_{9\text{-H}}/k_{9\text{-D}}$ ) is calculated as 1.36 ( $\Delta\Delta G_9^\ddagger = -0.182$  kcal/mol). The sum of these energy differences is necessarily equal to the difference of the energies of the isotopomeric TSs for OAr migration relative to the free ethers (see Scheme 1;  $\Delta\Delta G^\ddagger = \Delta\Delta G_8 + \Delta\Delta G_9^\ddagger = -0.856$

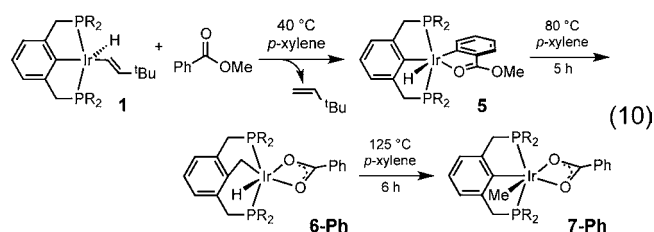


kcal/mol), corresponding to an overall calculated  $\text{KIE}_{\text{obs}}$  of 4.24. EIEs for alkane C–H addition at ambient temperature are typically<sup>81</sup> above 2.0 but our calculated value of  $\text{EIE}_8 = 3.12$  is unusually high. We attribute this to particularly low Ir–H(D) bending frequencies due to the shallow energy surface for deformation of the ligand arrangement in the equatorial plane of the five-coordinate  $d^6$  complex.<sup>82</sup> The value of 1.36 for  $\text{KIE}_9$  may seem high for a secondary KIE but is well preceded by organic  $\text{S}_{\text{N}}1$  (solvolysis) reactions for which values above 1.2 per H/D atom are common.<sup>83–90</sup> It seems quite plausible that OAr migration in eq 9 (KIE calculated as 1.17 per H/D) would afford a secondary KIE comparable to that resulting from the dissociation of oxygen-bound anions (e.g., tosylates) from the corresponding alkyl derivatives. Thus, the value of  $\text{KIE}_{\text{obs}}$ , 4.3(3), in conjunction with the DFT calculations, is supportive of the pathway of Scheme 2 with 1,2-aryloxide migration as the rate-determining step.

**2.1.3. Reactions of (PCP)Ir with Methyl Esters.** As with ethers, certain esters underwent clean oxidative addition of C–O bonds by (PCP)Ir. In all such cases, the stronger—and typically much less reactive—of the two ester C–O single bonds was cleaved, i.e., the alkoxy C–O bond, rather than the acyl C–O linkage.<sup>27,32,91–93</sup>

Since the acyl carbon lacks C–H bonds, this observation is of course consistent with a reaction mechanism related to that proposed for ethers and discussed above. Moreover, and in contrast with the ether additions, for some of the ester C–O addition reactions we have been able to observe and isolate apparent intermediates in a pathway initiated by C–H activation.

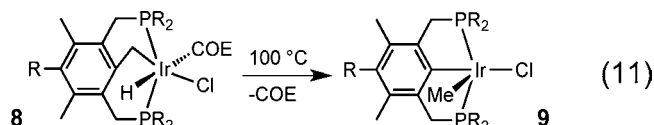
Addition of methyl benzoate (1.15 equiv.) to **1** in *p*-xylene- $d_{10}$  at room temperature resulted in the rapid formation of (PCP)Ir(H)[ $\kappa^2$ -(C<sub>6</sub>H<sub>4</sub>C(O)OMe)], **5**, the product of addition of the aryl C–H bond ortho to the ester group and coordination of the ester carbonyl oxygen (eq 10). The



structure of **5** was determined by NMR spectroscopy, most notably the presence of a signal in the <sup>1</sup>H NMR spectrum at  $\delta$  –9.24 ppm (<sup>2</sup>J<sub>PH</sub> = 18.1 Hz) indicative of a hydride coordinated *trans* to an aryl group.<sup>94</sup> The structure was confirmed by X-ray crystallography (Figure 2). The formation of complex **5** proceeds in analogy with the previously reported reaction of (PCP)Ir with acetophenone including, in particular, the selectivity for formation of the *trans*-C–H addition product,

which is indicative of C–H addition occurring prior to carbonyl oxygen coordination.<sup>94</sup>

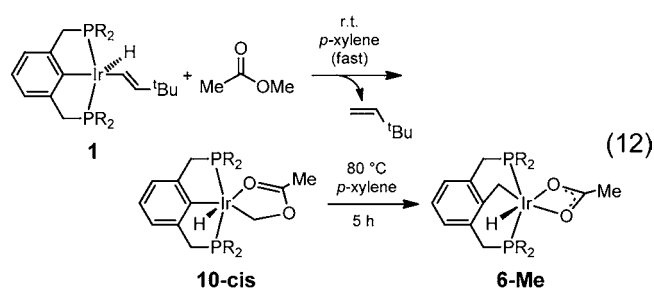
Quite surprisingly, heating the resulting solution of **5** at 80 °C for 5 h resulted in formation of **6-Ph**, in which a methylene unit derived from the carbomethoxy group has apparently inserted into the PCP aryl–Ir bond (eq 10). The Ir–CH<sub>2</sub>–Ar group of **6-Ph** gave rise to a triplet at  $\delta$  2.28 ppm (<sup>3</sup>J<sub>PH</sub> = 9.8 Hz) in the <sup>1</sup>H NMR spectrum, and a triplet at  $\delta$  –17.67 ppm (<sup>2</sup>J<sub>CP</sub> = 5.2 Hz) in the <sup>13</sup>C NMR spectrum. These values are similar to those reported by Milstein et al. for complex **8** (eq 11).<sup>95,96</sup> In the <sup>1</sup>H NMR spectrum the hydride appeared as a triplet at  $\delta$  –32.76 ppm (<sup>2</sup>J<sub>PH</sub> = 12.5 Hz). Single crystal X-ray analysis confirmed the structure of **6-Ph** (Figure 2).



Heating complex **6-Ph** at 125 °C in *p*-xylene for 9 h led to the formation of the methyl benzoate C(sp<sup>3</sup>)-O oxidative addition complex **7-Ph** (eq 10). The Ir–CH<sub>3</sub> signal of **7-Ph** appears as a triplet at  $\delta$  1.45 ppm (<sup>3</sup>J<sub>PH</sub> = 4.8 Hz) and as a triplet at  $\delta$  –29.1 ppm (<sup>2</sup>J<sub>CP</sub> = 4.6 Hz) in the <sup>1</sup>H and <sup>13</sup>C NMR spectra, respectively. Complex **7-Ph** was crystallized from *n*-hexane, and the structure was confirmed by X-ray crystallography (Figure 2).

Milstein has reported that complex **8**, with a (PCP-CH<sub>2</sub>)IrH motif analogous to that of **6-Ph**, affords the iridium methyl complex **9** upon heating (eq 11).<sup>95</sup> The formation of **7-Ph** from **6-Ph** can be explained analogously, as resulting from reductive elimination of (PCP–CH<sub>2</sub>) and H from **6-Ph**, followed by C–C bond cleavage to give complex **7-Ph**.

The room-temperature reaction of **1** with methyl acetate, like that with methyl benzoate, resulted in a cyclometalated product, but in contrast to the methyl benzoate reaction, C–H bond addition occurred at the carbomethoxy group, affording complex **10-cis** (eq 12). The hydride resonance of **10-**



*cis* appears in the <sup>1</sup>H NMR spectrum as a triplet (<sup>2</sup>J<sub>PH</sub> = 16.1 Hz) at  $\delta$  –25.98 ppm; this relatively upfield shift is consistent with the coordination geometry in which the hydride is *trans* to the ester carbonyl oxygen.<sup>94</sup> The resonances of the IrCH<sub>2</sub>O group appear at  $\delta$  67.19 ppm (t, <sup>2</sup>J<sub>PC</sub> = 6.6 Hz) in the <sup>13</sup>C NMR spectrum and 6.74 ppm (t, <sup>3</sup>J<sub>PH</sub> = 7.9 Hz, 2H) in the <sup>1</sup>H NMR spectrum, while a singlet attributable to the acetyl methyl group appears at  $\delta$  1.73 ppm in the <sup>1</sup>H NMR spectrum. Formation of complex **10-cis** is reversible at room temperature; when complex **10-cis-d<sub>3</sub>** was formed from the reaction of **1** with methyl acetate-*d*<sub>3</sub> (CH<sub>3</sub>CO<sub>2</sub>CD<sub>3</sub>), it underwent exchange upon treatment with an excess of perprotio methyl acetate to yield perprotio **10-cis**.

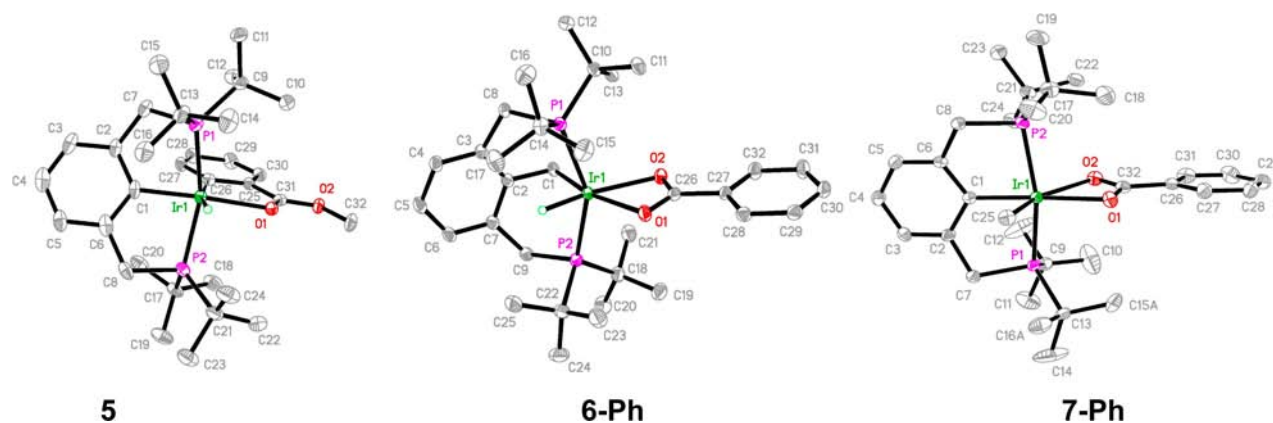


**Figure 2.** X-ray structures of  $(\text{PCP})\text{Ir}(\text{H})[\kappa^2\text{-(C}_6\text{H}_4\text{C(O)OMe)}]$  (**5**),  $(\text{PCP-CH}_2)\text{Ir}(\text{H})(\kappa^2\text{-O}_2\text{CPh})$  (**6-Ph**), and  $(\text{PCP})\text{Ir}(\text{CH}_3)(\kappa^2\text{-O}_2\text{CPh})$  (**7-Ph**).

Thermolysis of complex **10-cis** at 80 °C, like complex **5**, results in the formation of a product, **6-Me**, in which the  $\text{CH}_2$  group derived from the carbomethoxy group has inserted into the PCP aryl-Ir bond (eq 12). The Ir- $\text{CH}_2$ -Ar group of **6-Me** afforded triplets at  $\delta$  2.17 ppm ( $^3J_{\text{PH}} = 9.5$  Hz) in the  $^1\text{H}$  NMR spectrum and  $\delta$  -17.94 ppm ( $^2J_{\text{CP}} = 5.1$  Hz) in the  $^{13}\text{C}$  NMR spectrum, while the hydride gave rise to a  $^1\text{H}$  NMR signal at -32.90 ppm ( $J_{\text{PH}} = 12.5$  Hz). These diagnostic features are all clearly very similar to those found in the spectra of **6-Ph**, and the structure of **6-Me** was confirmed crystallographically (Figure 3).

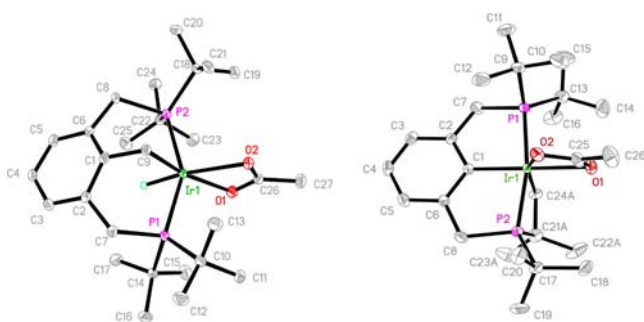
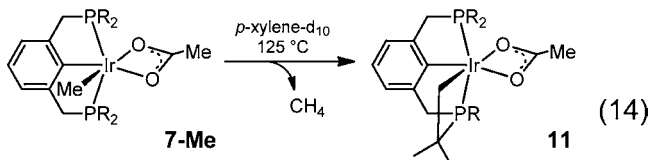
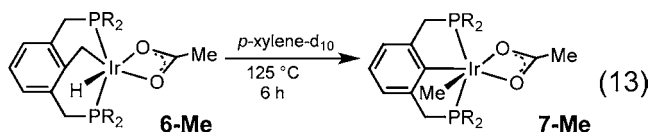


**Figure 3.** X-ray structures of  $(\text{PCP-CH}_2)\text{Ir}(\text{H})(\kappa^2\text{-O}_2\text{CMe})$  (**6-Me**) and cyclometalated  $(\text{PCP})\text{Ir}(\text{acetate})$ ,  $[(\kappa^4\text{-C}_6\text{H}_3\text{-2-(CH}_2\text{P}^t\text{Bu)-6-(CH}_2\text{P}^t\text{Bu(CMe}_2\text{CH}_2)))]\text{Ir}(\text{O}_2\text{CMe})$  (**11**).

Heating a *p*-xylene solution of **6-Me** at 125 °C produced **7-Me**, in analogy with the reaction of **7-Ph**, but this reaction was accompanied by formation of a coproduct **11** (eqs 13 and 14).



Complete conversion of **6-Me** yielded an approximately 1:1 mixture of **7-Me** and **11**. Complex **7-Me** showed a signal in the  $^1\text{H}$  NMR spectrum attributable to the iridium bound methyl group at  $\delta$  1.30 ppm (Ir- $\text{CH}_3$ ), as well as a singlet associated with the acetyl group at  $\delta$  1.82 ppm. Complex **11** was characterized by NMR spectroscopy and by X-ray crystallographic analysis of a crystal obtained by slow evaporation from a solution of **11** in hexanes (Figure 3).

In contrast with methyl benzoate and methyl acetate, methyl trifluoroacetate reacted rapidly with **1** at room temperature to give the methylene-bridged-PCP product  $(\text{PCP-CH}_2)\text{Ir}(\text{H})(\kappa^2\text{-O}_2\text{CCF}_3)$ , **6-CF₃**. Heating a  $\text{C}_6\text{D}_6$  solution of **6-CF₃** at 100 °C for 30 h gave the complex  $(\text{PCP})\text{Ir}(\text{CH}_3)(\text{O}_2\text{CCF}_3)$  (**7-CF₃**).

**2.1.4. Mechanism of Methyl Ester C–O Bond Addition.** A DFT study of the pathway for the reaction of methyl acetate with  $(\text{PCP})\text{Ir}$  was conducted. Two  $(\text{PCP})\text{Ir}/\text{CH}_3\text{CO}_2\text{Me}$  adducts were located (see Table S2 of the SI); in the lowest energy adduct, with  $G = -4.9$  kcal/mol (energy values are relative to methyl acetate plus free three-coordinate  $(\text{PCP})\text{Ir}$  unless indicated otherwise), the ester coordinates to Ir only through its carbonyl oxygen (Ir- $\text{O}_2(\text{carbonyl}) = 2.27$  Å, Ir- $\text{O}_1(\text{methoxy}) = 4.49$  Å). This precoordination of the substrate does not appear to play any particular role in the reaction pathway described below, other than possibly competing with  $(\text{PCP})\text{Ir}(\text{TBV})(\text{H})$  ( $G = -4.7$  kcal/mol) as the resting state; the structure of the adduct is unrelated to that of the TS for the subsequent C–H addition reaction.

The calculations (see Figure 4) indicate a low barrier to C–H addition, unassisted by either oxygen atom, followed by a facile chelation to give intermediate **10-cis**; the free energy of the TS is calculated to be 8.4 kcal/mol (relative to methyl acetate plus free three-coordinate  $(\text{PCP})\text{Ir}$ ), or 13.3 kcal/mol above the O-coordinated species (which is comparable to the energy of the  $(\text{PCP})\text{Ir}(\text{TBV})(\text{H})$  precursor). These values are consistent with the rapid formation of **10-cis** observed in the reaction of methyl acetate with a  $(\text{PCP})\text{Ir}$  precursor at room temperature.  $\alpha$ -Carboxylate migration from **10-cis** in a manner analogous to the  $\alpha$ -aryloxide migration that occurs with  $(\text{PCP})\text{Ir}(\text{H})(\text{CH}_2\text{OAr})$ , whereby the  $\alpha$ -oxygen migrates to give *cis*- $(\text{PCP})\text{Ir}(\text{H})(\text{CH}_2)(\text{O}_2\text{CMe})$ , is calculated to have a very high barrier, 33.2 kcal/mol ( $G_{\text{TS}} = 26.0$  kcal/mol relative to free  $(\text{PCP})\text{Ir}$  plus  $\text{MeCO}_2\text{Me}$ ). A much more facile migration of carboxylate from **10-cis** to afford *cis*- $(\text{PCP})\text{Ir}(\text{H})(\text{CH}_2)(\text{O}_2\text{CMe})$  proceeds via an electrocyclic transition state **TS-10-12-cis** (Scheme 3).

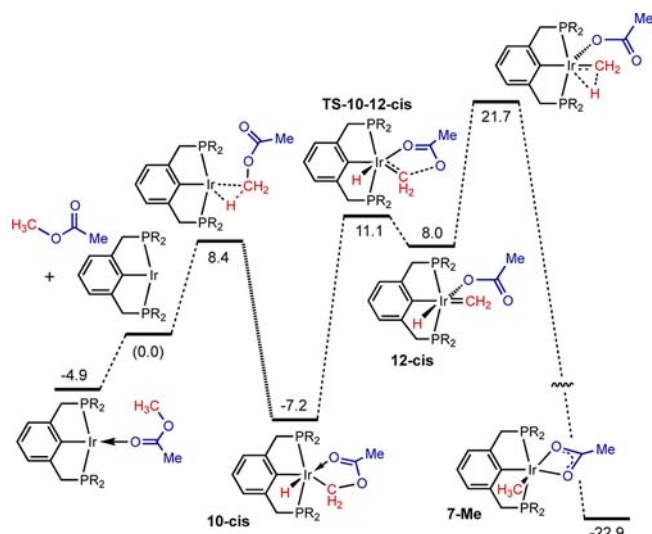


**Figure 4.** Calculated Gibbs free energies (kcal/mol) for reaction of (PCP)Ir and  $\text{CH}_3\text{-OAc}$  via a hypothetical “cis-pathway”. Values of  $G$  are given relative to free (PCP)Ir and  $\text{CH}_3\text{-OAc}$ . The free energies correspond to a reference state of 1 M concentration for each species participating in the reaction and  $T = 298.15$  K. Potential energies, enthalpies, entropies and free energies for (PCP)Ir +  $\text{CH}_3\text{-OAc}$  reactions are summarized in Table S2 of the SI.

This migration TS is very “late” in its structural parameters. The Ir–O2 (carbonyl oxygen) bond is preserved in the cyclic TS (Ir–O2 = 2.23 vs 2.25 Å in the product), while the C–O1 bond is effectively broken (2.92 Å in the TS vs 3.04 Å in the product). The Ir–C bond is very close to double bond length (1.925 vs 1.921 Å in the product), and the  $\text{CH}_2$  group has rotated ca.  $57^\circ$  toward its preferred “horizontal” orientation, i.e., in the plane of Ir and the nonphosphorus coordinating groups ( $\angle\text{H-Ir-C}(\text{CH}_2)\text{-H1} = 32^\circ$ ;  $\angle\text{H-Ir-C}(\text{CH}_2)\text{-H2} = -146^\circ$ ). The reaction coordinate at the TS shows substantial torsional motion of the  $\text{CH}_2$  and  $\text{O2C}(\text{O1})\text{Me}$  units in opposite directions. **TS-10-12-cis** is relatively low in free energy at  $G_{\text{TS}} = 11.1$  kcal/mol or only 3.1 kcal/mol above the methylidene complex to which it leads (**12-cis**); perhaps this is not surprising as this is effectively a “6-electron” retro-electrocyclization reaction. The resulting methylidene intermediate, **12-cis**, is at  $G = 8.0$  kcal/mol, or 15.2 kcal/mol above the free energy of **10-cis**, and thus this reaction is quite reversible (Figure 4).

Subsequent to the five-membered cyclic carboxylate migration, migration of the hydride to methylidene would produce the observed C–O oxidative addition product; this hydride migration has  $G_{\text{TS}} = 21.7$  kcal/mol (26.6 kcal/mol above the (PCP)Ir/ester adduct). However, while this “cis-pathway”, as shown in Figure 4, offers a fairly low barrier to the final C–O addition product, it does *not* account for the initial

formation of  $(\text{PCP-CH}_2)\text{Ir}(\text{H})(\text{O}_2\text{CMe})$ , which is observed prior to the C–O addition product.

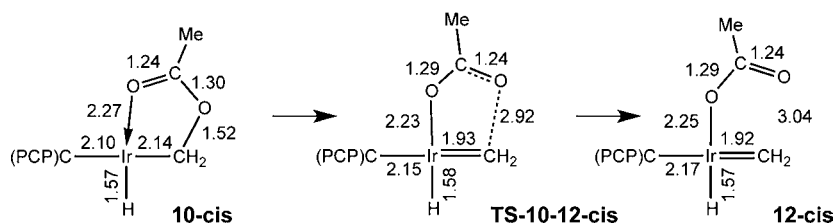
Rotation by  $180^\circ$  around the Ir– $\text{CH}_2\text{OAc}$  bond of **10-cis** can lead to an isomer, **10-trans**, in which H and the Ir-coordinated  $\text{CH}_2\text{OAc}$  carbon are situated mutually trans. Although we have not been able to locate a proper TS (i.e., a stationary point on the PES with just one negative eigenvalue of the Hessian matrix) for this process, constrained dihedral angle optimizations indicate that the potential energy barrier separating the  $\text{cis}_{\text{H-CH}_2}$  complex **10-cis** from **10-trans** is less than 14 kcal/mol, and isomerization should therefore be facile. Alternatively, loss of methyl acetate from **10-cis** has a calculated barrier of 15.6 kcal/mol (consistent with the facile exchange noted above and observed with **10-cis-d<sub>3</sub>** and  $\text{CH}_3\text{CO}_2\text{CH}_3$ ); rapid readdition of the C–H bond to (PCP)Ir, followed by collapse of the C–H addition product to produce **10-trans** would thus have an overall barrier of only 15.6 kcal/mol.

The geometries of the five-membered Ir–C–O–C=O rings in **10-cis** and **10-trans** (Scheme 4) are quite similar, with slightly longer distances in each case for the respective bond trans to the hydride versus trans to the PCP ipso carbon (calculated Ir–C bond lengths (Å) are 2.144 and 2.166, while Ir–O bond lengths are 2.272 and 2.255 in **10-cis** and **10-trans**, respectively). **10-trans** is higher in energy than **10-cis** by 5.6 kcal/mol, in accord with the fact that this isomer is not observed experimentally. This cis-trans conformer energy difference could arise because in **10-trans** the coordinating group of the chelate with the much stronger trans-influence (the oxymethylene carbon versus the carbonyl oxygen) is positioned trans to the strong trans-influence hydride ligand.

The calculated barrier for  $\alpha$ -carboxylate migration from **10-trans** is very high ( $G_{\text{TS}} = 31.4$  kcal/mol), whereas cyclic carboxylate migration is calculated to occur with a modest barrier ( $G_{\text{TS}} = 14.5$  kcal/mol), leading to *trans*-(PCP)Ir(H)-(CH<sub>2</sub>)(O<sub>2</sub>CMe) (**12-trans**, Figure 5). The corresponding transition state, **TS-10-12-trans** (Scheme 4), is structurally very similar to **TS-10-12-cis** (Scheme 3); for example, it is very “late” in its geometrical parameters and the  $\text{CH}_2$  unit is significantly rotated toward the “horizontal” plane (Scheme 4;  $\angle\text{C}(\text{PCP})\text{-Ir-C}(\text{CH}_2)\text{-H1} = 42^\circ$ ;  $\angle\text{C}(\text{PCP})\text{-Ir-C}(\text{CH}_2)\text{-H2} = -144^\circ$  in TS). Subsequent hydride migration to the methylidene unit, however, is of course not possible in the case of the trans isomer.

While hydride-to-methylidene migration is not geometrically possible for methylidene complex **12-trans**, the barrier to migration of the PCP aryl group to the methylidene (i.e., methylidene insertion into the Ir–C(ipso) bond) is quite low, 7.5 kcal/mol ( $G_{\text{TS}} = 17.8$  kcal/mol; Figure 5). This step yields the experimentally observed species **6-Me** and is very exergonic ( $\Delta G = -30.0$  kcal/mol); therefore, this step is effectively irreversible as the back reaction has a calculated barrier  $G^\ddagger = 37.5$  kcal/mol. The rate determining step for the reaction of **10-**

**Scheme 3**





Scheme 4

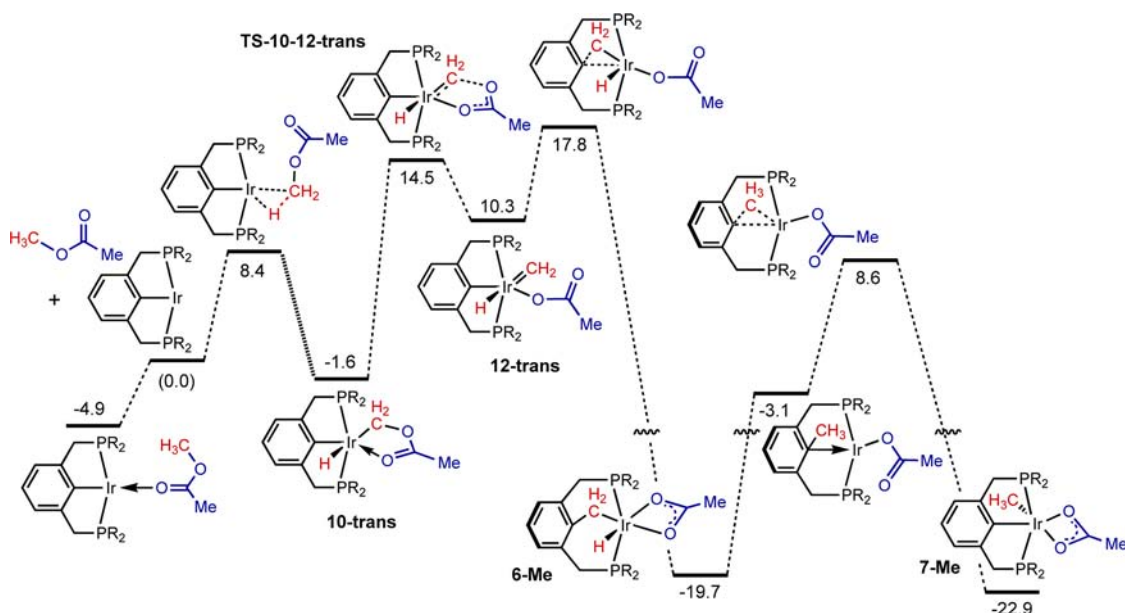
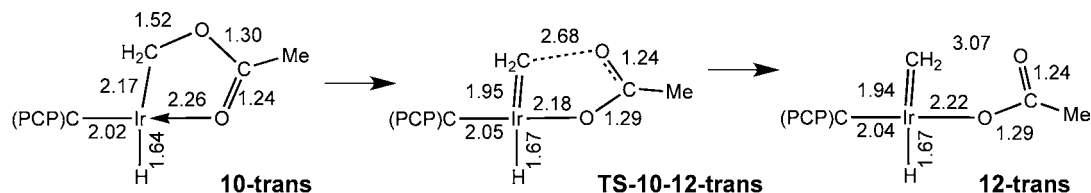
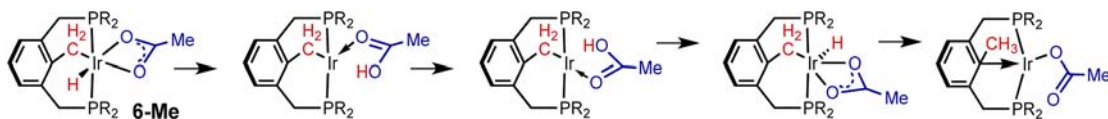


**Figure 5.** Calculated Gibbs free energies (kcal/mol) for reaction of (PCP)Ir and  $\text{CH}_3\text{-OAc}$  via the “trans-pathway”, which is proposed to be the actual reaction path (as opposed to the hypothetical “cis-pathway” shown in Figure 4). Values of  $G$  are given relative to free (PCP)Ir and  $\text{CH}_3\text{-OAc}$ . The free energies correspond to a reference state of 1 M concentration for each species participating in the reaction and  $T = 298.15$  K. Potential energies, enthalpies, entropies and free energies for (PCP)Ir +  $\text{CH}_3\text{-OAc}$  reactions are summarized in Table S2 of the SI.

Scheme 5

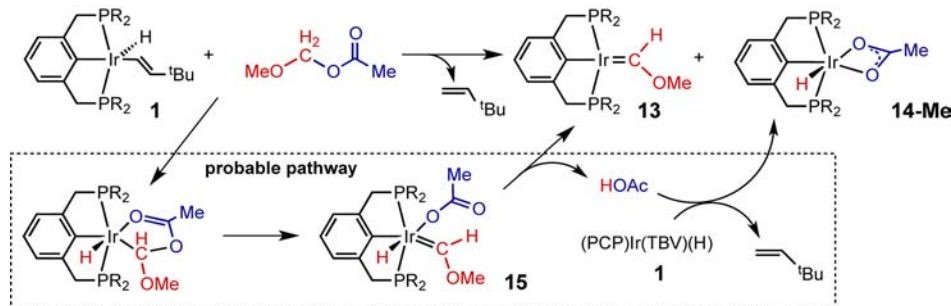


cis to give **6-Me** (eq 12) thus appears to be this aryl-to-methylene migration (occurring via a reversible isomerization to **10-trans**); the overall barrier (from **10-cis** for which  $G = -7.2$  kcal/mol) via this “trans-pathway” is calculated to be approximately 25 kcal/mol. This is in excellent agreement with experiment, which indicates an activation barrier of ca. 27 kcal/mol (a half-life of 1 h at 80 °C corresponds to  $\Delta G^\ddagger = 26.8$  kcal/mol).

(PCP- $\text{CH}_3$ )Ir( $\text{O}_2\text{CMe}$ ), the product of C–H reductive elimination from (PCP- $\text{CH}_2$ )Ir(H)( $\text{O}_2\text{CMe}$ ) (**6-Me**) is calculated to be *thermodynamically* quite accessible with  $G = -3.1$  kcal/mol (Figure 5). We have searched extensively for a TS of reasonably low energy for this C–H reductive elimination from (**6-Me**). If the coordination sphere around Ir is otherwise kept intact, then the computed barrier for direct C–H elimination is calculated to be exceedingly high,  $G_{\text{TS}} = 32.1$  kcal/mol; since  $G_{\text{6Me}} = -19.7$  kcal/mol, this implies a barrier  $\Delta G^\ddagger \approx 52$  kcal/mol. A pathway in which a phosphine group is detached from the Ir center offers a TS that is of considerably lower energy,  $G_{\text{TS}} \approx 17$  kcal/mol ( $\Delta G^\ddagger \approx 37$  kcal/mol), but this is still quite high. The calculations reveal a lower

energy pathway (Scheme 5 and Table S2 of the SI), however, in which the hydride undergoes trans-migration prior to C–H elimination. This proceeds via O–H elimination to give a coordinated acetic acid ligand which can rotate around the Ir–O(carbonyl) bond and then undergo O–H addition (Scheme 5). The TS for the initial protonation of acetate (O–H elimination) has a free energy  $G_{\text{TS}} = 7.9$  kcal/mol ( $\Delta G^\ddagger = 27.6$  kcal/mol). A series of constrained dihedral angle optimizations (angle Ir–O–C–OH was varied) indicate that rotation of the acetic acid about the Ir–O bond may be accomplished via a TS with  $G_{\text{TS}} \approx 11$  kcal/mol, while for the subsequent O–H addition,  $G_{\text{TS}} = -5.6$  kcal/mol. (As the rotation involves a presumably very acidic O–H group, the gas-phase calculated energy for this process should perhaps be viewed as an upper limit.) C(PCP- $\text{CH}_2$ )-H elimination from the resulting isomer is facile ( $G_{\text{TS}} = 4.7$  kcal/mol; Table S2 of the SI), giving (PCP- $\text{CH}_3$ )Ir( $\text{O}_2\text{CMe}$ ). Oxidative addition of the PCP- $\text{CH}_2$  C–C bond addition in (PCP- $\text{CH}_3$ )Ir( $\text{O}_2\text{CMe}$ ) yields the final product, **7-Me**; the TS for this reaction is at 8.6 kcal/mol relative to the free reactants. Thus, the highest energy TS for the overall process is calculated to be no more than ca. 11 kcal/

Scheme 6. Formation of a Carbene Complex from the Reaction of (PCP)Ir with Methoxymethyl Acetate and Probable Reaction Pathway



mol (if acetic acid rotation is rate-limiting) but no less than 8.6 kcal/mol (if C–C addition is rate-limiting). The overall barrier for transformation of **6-Me** ( $G = -19.7$  kcal/mol) to the observed C–O addition product **7-Me** is therefore calculated to be in the range from 28 to 31 kcal/mol. This is in very good agreement with the experimental observation that the reaction proceeds to completion in several hours at 125 °C (a half-life of 1 h at 125 °C corresponds to  $\Delta G^\ddagger = 30.3$  kcal/mol).

**2.1.5. Observation of a Model Carbene Complex.** In an effort to observe the key carbene complex intermediate, we studied the reaction of (PCP)Ir with methoxymethyl acetate, MeOCH<sub>2</sub>OAc, anticipating that the presence of a methoxy group could potentially stabilize the methyldene intermediate. When a half equivalent of MeOCH<sub>2</sub>OAc was treated with (PCP)Ir(TBV)(H) (**1**) at room temperature, the formation of (PCP)Ir=C(H)(OMe) (**13**) and (PCP)Ir(H)(OAc) (**14-Me**) was observed in approximately a 1:1 ratio (Scheme 6). Although we were not able to separate complex **13** from the product mixture, complete NMR characterization of **13** was possible, since analytically pure **14-Me** could be prepared from the reaction of **1** with ethyl acetate (vide infra). As a diagnostic feature, the Ir=C–H resonance appears at  $\delta$  14.89 ppm as a triplet in the <sup>1</sup>H NMR spectrum and  $\delta$  254.8 ppm in the <sup>13</sup>C NMR spectrum, chemical shifts very similar to the resonances reported for other iridium Fischer-type carbene complexes.<sup>69,97,98</sup> The formation of both products **13** and **14-Me** is presumably attributable to the formation of a half equivalent of hydrido acetate carbene complex (**15** or its *cis* isomer). This methoxy-stabilized analogue of **12** does not undergo phenyl-to-carbene (or hydride-to-carbene) migration but instead eliminates acetic acid, which rapidly reacts with remaining **1** to afford **14-Me**.

**2.1.6. Reaction of (PCP)Ir with Methyl Tosylate and Mechanism.** Methyl tosylate (CH<sub>3</sub>OTs) also reacts with (PCP)Ir to undergo oxidative addition of the sp<sup>3</sup> C–O bond. When 1.1 equiv. of CH<sub>3</sub>OTs was added to a *p*-xylene solution of **1** at room temperature, an immediate color change from dark to bright red was observed. The reaction produces a quantitative yield of (PCP)Ir(CH<sub>3</sub>)(OTs) (**16**), whose structure was confirmed by NMR spectroscopy as well as X-ray crystallography (eq 15, Figure 6). Resonances attributable

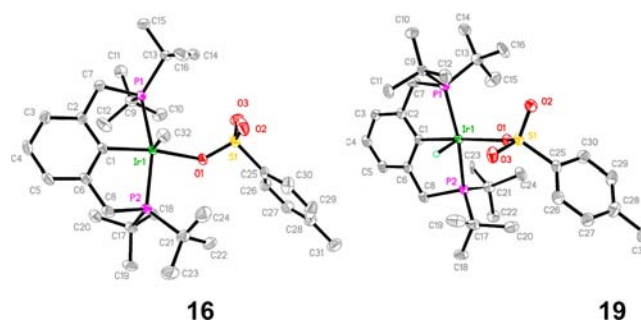
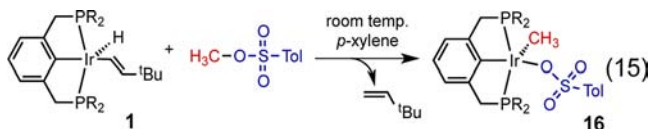
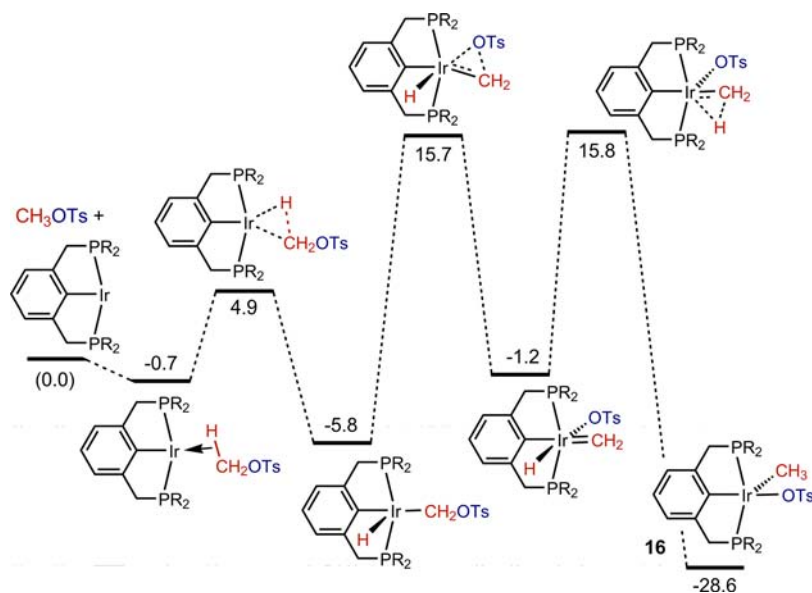


Figure 6. X-ray structures of (PCP)Ir(Me)(OTs) (**16**) and (PCP)Ir(H)(OTs) (**19**).

to the Ir–CH<sub>3</sub> group in **16** appear at  $\delta$  2.19 ppm (t,  $J_{\text{PH}} = 5.0$  Hz) in the <sup>1</sup>H NMR spectrum and at  $\delta$  –25.4 ppm in the <sup>13</sup>C NMR spectrum, positions similar to the resonances observed in complexes **4** and **7**.

A facile pathway for reaction 14 is calculated, analogous to the  $\alpha$ -aryloxy migration mechanism for CH<sub>3</sub>–OAr addition. The computed free energy profile is presented in Figure 7. A direct C–O addition mechanism is calculated to have a much higher barrier with  $G_{\text{TS}} = 37.5$  kcal/mol. The free-energy profile shown in Figure 7 (more detailed energetics are presented in Table S3 of the SI) is quite similar to that calculated for oxidative addition of the C–O bond of *p*-CH<sub>3</sub>–OC<sub>6</sub>F<sub>4</sub>Me (Figure 1). Reaction 14 affording (PCP)Ir(CH<sub>3</sub>)(OTs) is slightly more exergonic ( $G = -28.6$  kcal/mol) than the analogous reaction with *p*-MeOC<sub>6</sub>F<sub>4</sub>Me ( $G = -26.4$  kcal/mol). The barriers for  $\alpha$ -OTs migration and 1,2-H migration are computed as essentially equal ( $G_{\text{TS}} = 15.7$  and 15.8 kcal/mol, respectively). The overall barrier is calculated as 21.5 or 21.6 kcal/mol, respectively, consistent with the experimentally observed rapid rate of reaction at ambient temperature.

In analogy to the experiments with methyl aryl ethers, the H/D kinetic isotope effect for oxidative addition of methyl tosylate to (PCP)Ir was measured. When a mixture of CH<sub>3</sub>OTs and CD<sub>3</sub>OTs (at least 10-fold excess of each) was treated with (PCP)Ir(TBV)(H) in *p*-xylene solution, two singlets, attributable to (PCP)Ir(CH<sub>3</sub>)(OTs) (**16**) and (PCP)Ir(CD<sub>3</sub>)(OTs) (**16-d<sub>3</sub>**) were observed in the <sup>31</sup>P NMR spectrum. From an average of three such experiments the isotope effect was determined to be  $\text{KIE}_{\text{obs}} = k_{\text{CH}_3\text{OTs}}/k_{\text{CD}_3\text{OTs}} = 2.4(2)$ . As with the methyl aryl ether, the observed isotope effect is quite significant and clearly indicates that C–H bond activation is involved in or prior to the rate-determining step of oxidative C–O bond addition. The DFT-calculated overall KIE resulting from trideuteration (OCH<sub>3</sub> → OCD<sub>3</sub>) is 2.9 if  $\alpha$ -OTs



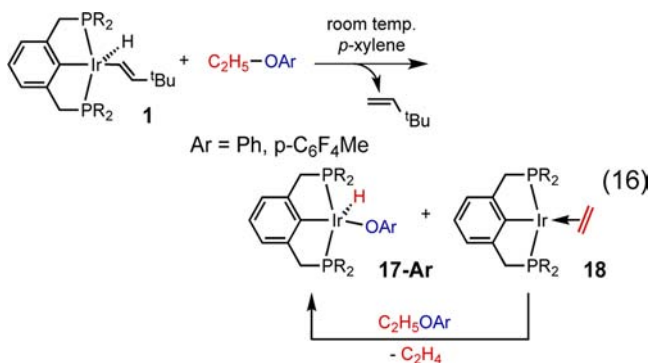
**Figure 7.** Calculated Gibbs free energies (kcal/mol) for reaction of (PCP)Ir and  $\text{CH}_3\text{-OTs}$ . Values of  $G$  are given relative to free (PCP)Ir and  $\text{CH}_3\text{-OTs}$ . The free energies correspond to a reference state of 1 M concentration for each species participating in the reactions and  $T = 298.15$  K. Potential energies, enthalpies, entropies, and free energies for (PCP)Ir +  $\text{CH}_3\text{-OTs}$  reactions are summarized in Table S3 of the SI.

migration is the rate-determining step, as opposed to 6.7 if hydride-migration to the carbene intermediate is the rate-determining step. The experimentally determined value of  $k_{\text{CH}_3}/k_{\text{CD}_3} = 2.4(2)$  is clearly in good agreement with the former case and, accordingly, we propose that  $\alpha\text{-OTs}$  migration is the rate-determining step for reaction 14.

## 2.2. Reactions of (PCP)Ir with Higher Alkyl Oxygenates R-OAr, R-OTs, and R-OAc (R = ethyl or isopropyl).

### 2.2.1. 1,2-H-OR Elimination Reactions (R = Ar, Ac, and Ts).

Reactions of aryl ethers, esters, and tosylate bearing alkyl groups higher than methyl have also been investigated. Treatment of 1 equiv. of ethyl phenyl ether with (PCP)Ir(TBV)(H) (**1**) at room temperature initially produced a mixture of intermediates resulting from C-H bond activation of the ether phenyl group. After approximately five hours at room temperature, this mixture was converted to an equimolar mixture of (PCP)Ir(H)(OPh) (**17-Ph**) and (PCP)Ir( $\text{C}_2\text{H}_4$ ) (**18**) (eq 16). Upon heating this mixture at 125 °C for two

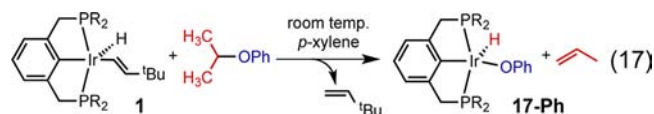


days, full conversion to (PCP)Ir(H)(OPh) was observed (eq 16). The structure of **17-Ph**, previously reported by our group,<sup>64,99</sup> was determined by NMR spectroscopy and X-ray crystallography.

In the case of 4-ethoxy-2,3,5,6-tetrafluorotoluene, the analogous reaction, at room temperature, immediately affords (PCP)Ir(H)(2,3,5,6-tetrafluoro-4-methyl phenoxide) (**17-**

**C<sub>6</sub>F<sub>4</sub>Me**) and **18** in a 1:1 ratio. Upon thermolysis of this reaction mixture at 80 °C for two days, **18** is fully converted to **17-C<sub>6</sub>F<sub>4</sub>Me** (eq 16).<sup>64</sup>

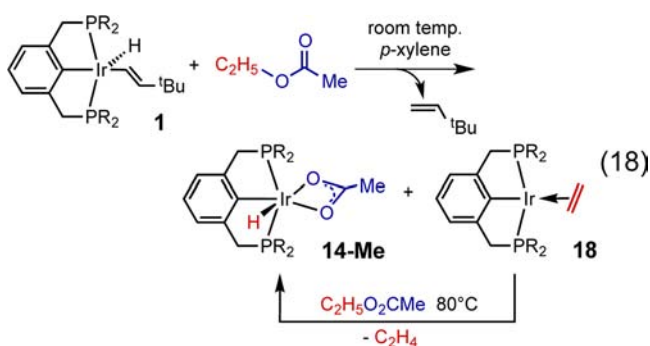
(PCP)Ir(TBV)(H) (**1**) also reacts with isopropyl phenyl ether to produce (PCP)Ir(H)(OPh) (**17-Ph**) and propene (eq 17); **17-Ph** was identified by <sup>31</sup>P NMR spectroscopy, and propene was identified by <sup>1</sup>H NMR spectroscopy and GC analysis.



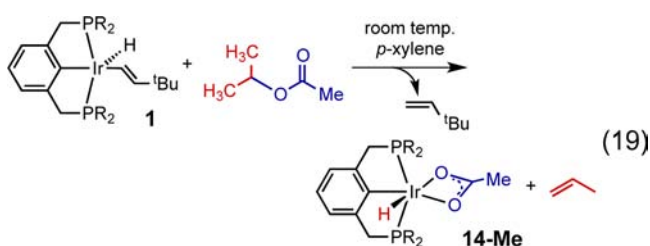
Somewhat surprisingly, however, the reaction of (PCP)Ir with *n*-propyl phenyl ether does not proceed at room temperature, even after three days. At 60 °C, **17-Ph** is formed but in only ~30% yield along with a complex mixture of byproducts. Likewise, the reaction with *n*-butyl phenyl ether requires heating to 60 °C and does not proceed cleanly, giving **17-Ph** in a yield of ca. 50%. In both cases, (PCP)IrH<sub>2</sub> was observed as a side product in the course of the reaction, probably generated by dehydrogenation of the alkyl chain of the alkyl phenyl ethers.

Addition of ethyl acetate to a *p*-xylene solution of (PCP)Ir(TBV)(H) (**1**) at room temperature resulted in an immediate color change from dark red to brown. <sup>31</sup>P and <sup>1</sup>H NMR spectroscopy revealed formation of an equimolar mixture of (PCP)Ir(H)(OAc) (**14-Me**) and (PCP)Ir(ethylene) (**18**). Upon further heating of the reaction mixture at 80 °C, **18** was converted to **14-Me** and ethylene (eq 18). The structure of **14-Me** was confirmed by X-ray crystallography (Figure S-8 of the SI) and NMR spectroscopy. The phosphorus resonance in the PCP ligand appears at  $\delta$  60.4 ppm as a doublet in the <sup>31</sup>P NMR spectrum, and Ir-H manifests at  $\delta$  -29.8 ppm as a triplet in the <sup>1</sup>H NMR spectrum.

The reaction of **1** with ethyl benzoate proceeded analogously to give **14-Ph** (see SI for spectroscopic and crystallographic characterization, Figure S-9 of the SI), but went to completion

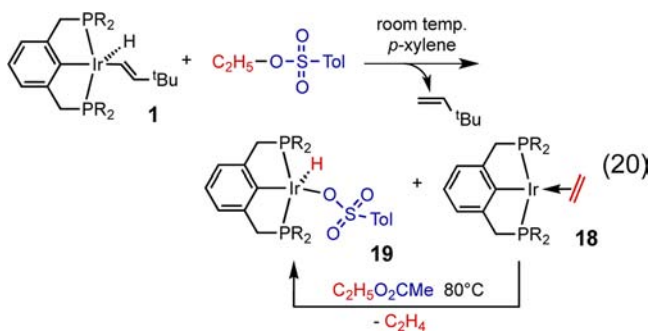


at room temperature (3 h). Compound **1** rapidly reacted with isopropylacetate to give complete conversion to **14-Me** and propene (eq 19). Presumably, the lesser stability of the propene analogue of **18** allows it to quickly react with isopropylacetate.



The reaction of **1** with *n*-propylacetate, in contrast, did not quickly lead to (PCP)Ir(H)(OAc). (PCP)IrH<sub>2</sub> and several unidentified intermediates were observed in the course of the reaction, although after ca. 20 h at room temperature **14-Me** was the only observed product. Other alkyl acetates underwent dehydrocarboxylation as indicated in Scheme 7, although yields were lower than those obtained with ethyl- or isopropylacetate.

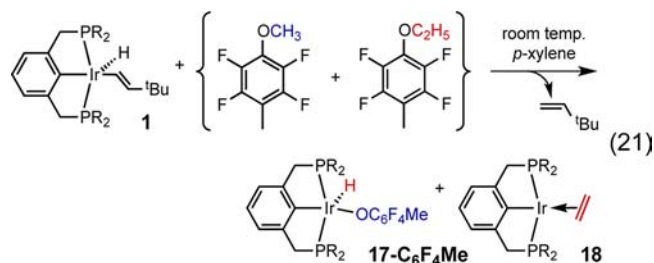
Analogously to the reactions with ethyl aryl ether or ethyl acetate (eqs 16 and 18) the reaction of **1** with ethyl tosylate gave an equimolar mixture of (PCP)Ir(H)(OTs) (**19**) and **18** (eq 20). The reaction went cleanly to completion immediately



at room temperature. The structure of **19** was determined by NMR spectroscopy and X-ray crystallography (Figure S-11 of the SI). Upon further heating of the reaction mixture at 80 °C for several hours, **18** was converted to **19**.

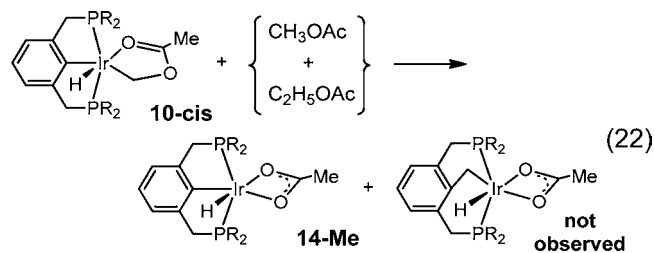
**2.2.2. Mechanistic Study of 1,2-H-OR Elimination Reactions (R = Ar, Ac, and Ts).** A priori, the above-described reactions of ethyl and higher alkyl aryl ethers, acetates and tosylate could proceed via direct C–O bond addition, followed by β-H elimination of the resulting alkyl group. In light of the results of the computational and mechanistic studies of the methyl derivatives, however, this would seem unlikely; this conclusion is reinforced by the results of experiments described below.

When a mixture of 4-methoxy-2,3,5,6-tetrafluorotoluene and 4-ethoxy-2,3,5,6-tetrafluorotoluene was reacted with (PCP)Ir (eq 21), aryloxide and ethylene complexes **17-C<sub>6</sub>F<sub>4</sub>Me** and **18**



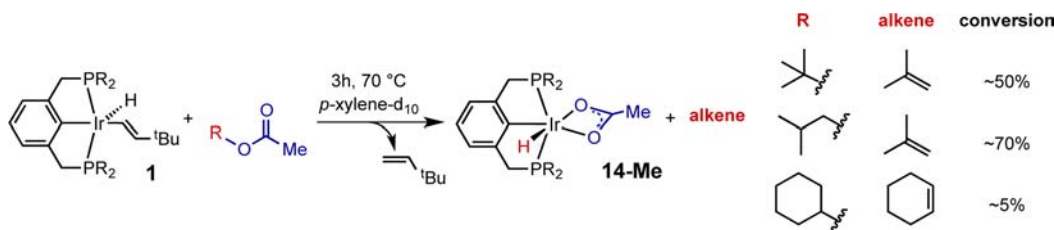
were formed exclusively (the same products that are obtained from pure 4-ethoxy-2,3,5,6-tetrafluorotoluene). There was no evidence of any reaction with 4-methoxy-2,3,5,6-tetrafluorotoluene.<sup>100</sup>

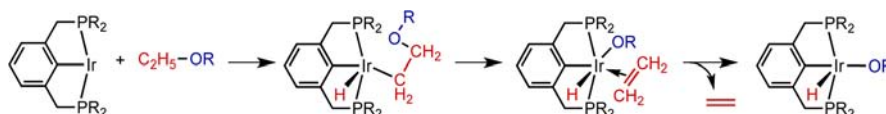
Closely related to the experiment of eq 21 with ethers, addition of an excess of a methyl acetate/ethyl acetate solution to a *p*-xylene solution of complex **10-cis** at room temperature resulted exclusively in the immediate formation of **14-Me** and **18** (eq 22), i.e., the same products that result from the reaction



of pure ethyl acetate. This implies, first, that the methyl acetate C–H addition is reversible, in accord with the calculated energy barriers (Figures 4 and 5) as well as the isotope exchange experiment between **10-cis-d<sub>3</sub>** and perprotio methyl acetate. The fact that ethyl acetate and ethyl aryl ether are so much more reactive than their methyl analogues argues strongly

Scheme 7. Reaction of (PCP)Ir with Alkyl Acetates



Scheme 8. Proposed Mechanism for 1,2-H-OR Elimination of Ethyl Oxygenates ( $R = \text{Aryl, Tosyl, and Acyl}$ )

against pathways involving direct C–O oxidative addition; it would seem improbable that direct addition of an O–CH<sub>3</sub> bond would be much less facile than O–C<sub>2</sub>H<sub>5</sub> addition. Moreover, a direct C–O addition would certainly not explain why *n*-propyl acetate and ether, but not the *i*-propyl analogues, are much less reactive than their ethyl analogues.

The high level of reactivity of the ethyl and *i*-propyl species can be explained with a pathway which, like the reactions of the methyl species, is initiated by C–H addition at a methyl group, but is then followed by  $\beta$ -oxygenate elimination. The analogous pathway for *n*-propylacetate, *n*-propyl phenyl ether, and *n*-butyl phenyl ether would require addition of a secondary C–H bond, which is less favorable for transition metal complexes in general,<sup>38</sup> and for (PCP)Ir in particular.<sup>55</sup> These results are thus all consistent with the pathway shown in Scheme 8 for the 1,2-H–OR eliminations.<sup>101,102</sup> A similar mechanism has been proposed by Chirik et al. in the reaction between a bis(indenyl) zirconium complex and diethyl ether, resulting in an equimolar mixture of Zr(H)(OEt) and Zr(ethylene) complexes.<sup>101</sup>

The apparent generally greater reactivity of the ethyl vs methyl oxygenates may be explained by generally greater ease of  $\beta$ - versus  $\alpha$ -oxygen elimination. Direct comparison between the rates of  $\alpha$ - and  $\beta$ -oxygen elimination are rare. However, Brookhart and co-workers have reported<sup>103</sup> that a Ni complex bearing a  $\beta$ -acetate group decomposes at  $-34$  °C via acetate elimination, while a similar Ni complex with an  $\alpha$ -acetate moiety is stable up to much higher temperature ( $>70$  °C). They also reported that a Pd complex with an  $\alpha$ -acetate substituted methyl group decomposed at a higher temperature than the analogous compound with an  $\alpha$ -trifluoroacetate ( $60$  °C vs  $10$  °C).<sup>103</sup> This finding is consistent with our result that (PCP)Ir effects C–O oxidative addition of methyl trifluoroacetate at room temperature, whereas the acetoxyethyl iridium complex (**10**) formed from the reaction with methyl acetate requires much higher temperature ( $70$  °C) to undergo further reaction.

In accord with the above discussion, the barrier to direct C(sp<sup>3</sup>)–O addition calculated for ethoxybenzene is prohibitively high,  $\Delta G_{\ddagger}^{\ddagger}_{\text{C-O}} = 40.8$  kcal/mol (ca. 46 kcal/mol relative to **1**). For 4-ethoxy-2,3,5,6-tetrafluorotoluene the calculated barrier is somewhat lower, but still very high,  $\Delta G_{\ddagger}^{\ddagger}_{\text{C-O}} = 35.0$  kcal/mol (ca. 40 kcal/mol relative to **1**). In contrast, the activation energy barriers are much lower for a reaction pathway (Figure 8) initiated by addition of a terminal sp<sup>3</sup> C–H bond from the ethoxy unit, followed by  $\beta$ -aryloxy elimination (more detailed energetics are presented in Table S4 of the SI). The computed C–H activation barrier heights for the fluorinated and parent substrates are virtually identical ( $\Delta G_{\ddagger}^{\ddagger} = 9.7$  and  $9.8$  kcal/mol for ethoxybenzene and 4-ethoxy-2,3,5,6-tetrafluorotoluene, respectively). The energies of the  $\beta$ -aryloxy migration transition states, however, are strongly reduced by the fluorine substituents on the aryl ring:  $\Delta G_{\text{TS}} = 14.0$  kcal/mol for ethoxybenzene vs  $7.6$  kcal/mol for 4-ethoxy-2,3,5,6-tetrafluorotoluene. This large difference in TS energies is apparently driven by an even larger difference in energies of the  $\beta$ -elimination products,  $G = -7.5$  kcal/mol and  $-17.2$  kcal/mol

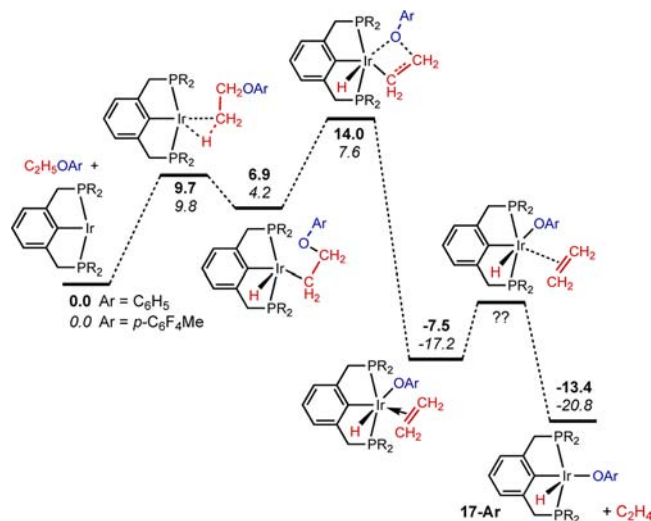


**Figure 8.** Calculated Gibbs free energies (kcal/mol) for reactions of (PCP)Ir and C<sub>2</sub>H<sub>5</sub>–OAr, Ar = phenyl (**bold**) and *p*-C<sub>6</sub>F<sub>4</sub>Me (*italics*). Values of  $G$  are given relative to free (PCP)Ir and C<sub>2</sub>H<sub>5</sub>–OAr, Ar = phenyl (**bold**) and *p*-C<sub>6</sub>F<sub>4</sub>Me (*italics*). The free energies correspond to a reference state of 1 M concentration for each species participating in the reactions and  $T = 298.15$  K. Potential energies, enthalpies, entropies and free energies for (PCP)Ir + C<sub>2</sub>H<sub>5</sub>–OAr, Ar = phenyl and *p*-C<sub>6</sub>F<sub>4</sub>Me, reactions are summarized in Table S4 of the SI.

for the phenoxide and 2,3,5,6-tetrafluoro-4-methylphenoxide, respectively. The binding enthalpies of the resulting coordinated ethylene are modest (9.0 and 10.3 kcal/mol for ethoxybenzene and 4-ethoxy-2,3,5,6-tetrafluorotoluene, respectively) and loss of ethylene is a slightly exergonic process ( $\Delta G_{\text{C}_2\text{H}_4\text{-loss}} = -5.9$  and  $-3.6$  kcal/mol for ethoxybenzene and 4-ethoxy-2,3,5,6-tetrafluorotoluene, respectively). A conventional TS for ethylene loss could not be located on the potential energy surface; however, the barriers may be very approximately estimated by equating barrier heights with binding enthalpies. This procedure leads to approximate  $G_{\text{TS,C}_2\text{H}_4\text{-loss}}$  free energies of 1.6 and  $-6.9$  kcal/mol for ethoxybenzene and 4-ethoxy-2,3,5,6-tetrafluorotoluene, respectively, values which are significantly lower than the preceding TSs.

The computed reaction energy profile for the reaction of ethyl acetate with (PCP)Ir is shown in Figure 9 (more detailed energetics are presented in Table S5 of the SI). The lowest TS for C–H addition has  $G_{\text{TS}} = 11.0$  kcal/mol relative to free reactants. Subsequent to C–H addition the carbonyl oxygen undergoes chelation to give the  $\kappa^2$ -acetoxyethyl hydride complex **20**.

Intermediate **20** ( $G = 4.1$  kcal/mol) undergoes  $\beta$ -acetate migration to give ethylene complex **21** with a TS that is only 12.0 kcal/mol above free reactants. The nature of TS-**20**–**21**, whose geometry is indicated in Scheme 9, is quite unusual. The C2–O1 bond is largely broken in TS-**20**–**21**, but unlike in a typical  $\beta$ -elimination TS, there is clearly no bonding developing between the iridium center and either C2 or O1. Indeed, although TS-**20**–**21** leads to an ethylene complex with typically

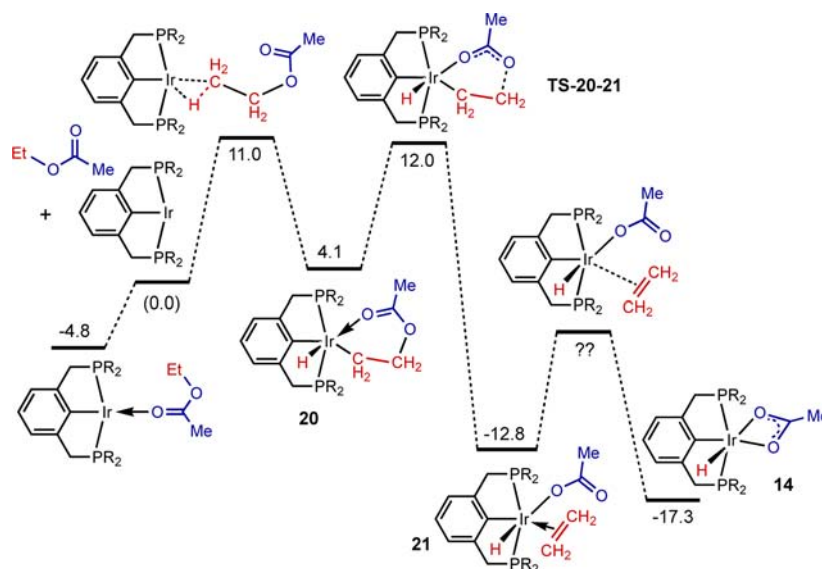
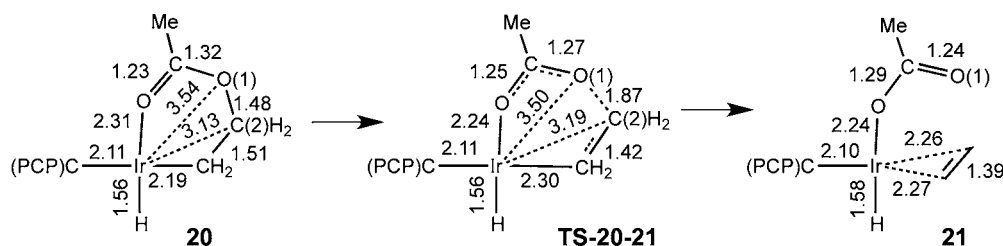


**Figure 9.** Calculated Gibbs free energies (kcal/mol) for reaction of (PCP)Ir and  $C_2H_5OAc$ . Values of  $G$  are given relative to free (PCP)Ir and  $C_2H_5OAc$ . The free energies correspond to a reference state of 1 M concentration for each species participating in the reactions and  $T = 298.15$  K. Potential energies, enthalpies, entropies, and free energies for reaction of (PCP)Ir and  $C_2H_5OAc$  are summarized in Table S5 of the SI.

**Scheme 9. Geometry of TS-20–21**



short Ir–C bond distances (2.26 Å for Ir–C2), the Ir–C2 distance in the TS is actually slightly longer, at 3.19 Å, than the distance of 3.13 Å found in the preceding intermediate, **20**. Following the intrinsic reaction coordinate leads toward the formation of an ethylene complex, although it is one in which the ethylene ligand is oriented in the “horizontal” plane (the plane containing the Ir atom and the three other non-phosphorus coordinating atoms); the ethylene unit in **21** is actually oriented along the P–Ir–P axis (perpendicular to the “horizontal” plane), presumably to reduce steric congestion in the “horizontal” plane. The free energy difference between the two conformers with different ethylene orientations is, however, only 1.2 kcal/mol.

Subsequent ethylene elimination from **21** is an exergonic, entropy-driven process ( $\Delta G_{\text{elim-C}_2\text{H}_4} = -4.5$  kcal/mol), and the ethylene binding enthalpy is fairly low ( $\sim 8.8$  kcal/mol). Despite a thorough geometrical search, we were not able to locate a conventional TS for ethylene loss from the (PCP)Ir unit on the potential energy surface. Given the weak binding however, the TS for ethylene loss is presumably much lower in energy than the preceding TS for acetate migration (TS-20–21, Figure 9). Thus acetate migration is presumably irreversible and is probably the rate-determining step. The overall barrier computed for reaction 17 in that case is only ca. 17 kcal/mol, consistent with the very rapid rate observed at room temperature.

### 3. CONCLUSIONS

Examples of  $C(sp^3)$ –O bond cleavage promoted by transition-metal complexes are limited despite expanding interest in this area. We find that (PCP)Ir oxidatively adds the  $C(sp^3)$ –O bond of various methyl oxygenates (esters, tosylates, and electron-poor aryl ethers). This reaction proceeds via C–H addition, followed by  $\alpha$ -OR migration (OR = OAr, OTs, OAc, or OC(O)Ar). In the case of OR = carboxylate, the  $\alpha$ -migration proceeds via a cyclic transition state in which the alkoxy group C–O bond is broken, while an Ir–C  $\pi$ -bond is formed and, formally, a dative Ir–O (carbonyl O) bond is converted to a covalent Ir–O bond. Derivatives with higher alkyl groups possessing  $\beta$ -C–H bonds react with (PCP)Ir to undergo a 1,2-dehydro-oxygenation to give (PCP)Ir(H)(OR) and the corresponding olefin. This reaction also is initiated by the addition of what is generally considered an “unreactive” C–H bond, in this case the C–H bond positioned  $\beta$  to the C–O bond undergoing cleavage; this is followed by  $\beta$ -oxygenate elimination. For the ethers and tosylates, the  $\beta$ -oxygenate elimination is apparently a straightforward process. In contrast, the TS for the acetates is a six-membered cyclic species in which the C–O bond is cleaved without any direct participation from the iridium center. On the basis of considerations of microscopic reversibility, the surprising mechanistic implications of this study presumably also apply to potential C–O bond-making reactions. Efforts to employ the principles elucidated in this work toward the development of catalytic processes are currently underway.

#### 4. COMPUTATIONAL METHODS

DFT calculations employed the recently developed M06 functionals;<sup>104</sup> an effective core potential and valence basis set of triple- $\zeta$  quality on the Ir atom (LANL08),<sup>105</sup> and basis sets of at least split valence plus polarization quality on all main group atoms.<sup>106</sup> The calculations were performed on the actual molecular species used in the experiments, i.e., truncations were not made to the substrates or to the (PCP)Ir fragment, which retained the bulky *t*-Bu groups on P. We did not consider solvent effects explicitly in the calculations, since all experiments were conducted in simple nonpolar hydrocarbons (e.g., *p*-xylene), and specific solvent dependence was not encountered in any of the experiments. Indeed, a few selected calculations in which the general effects of a surrounding solvent were included via a continuum dielectric model revealed only very minor changes in reaction barrier heights (<1 kcal/mol). A reference state of  $T = 298$  K and 1 M concentration of all reacting species was used. A complete description of the computational methodology is available in the SI.

#### ■ ASSOCIATED CONTENT

##### ● Supporting Information

Experimental details and procedures; spectral data for all complexes characterized; crystallographic structures and details for complexes **3h**, **3j**, **5**, **6-Ph**, **6-Me**, **7-Ph**, **11**, **14-Me**, **14-Ph**, **16**, and **19**; computational details, molecular energies, and geometries. This material is available free of charge via the Internet at <http://pubs.acs.org>.

#### ■ AUTHOR INFORMATION

##### Corresponding Author

alan.goldman@rutgers.edu; kroghjes@rutgers.edu

##### Notes

The authors declare no competing financial interest.

#### ■ ACKNOWLEDGMENTS

We thank David Laviska for helpful discussion regarding the aryl C–H addition reactions. We thank the National Science Foundation for support of this work through Grant CHE No. 1112456 and the Extreme Science and Engineering Discovery Environment (XSEDE), which is supported by National Science Foundation grant number OCI-1053575.

#### ■ REFERENCES

- (1) Lichtenthaler, F. W.; Mondel, S. *Pure Appl. Chem.* **1997**, *69*, 1853–1866.
- (2) Schlaf, M. *Dalton Trans.* **2006**, 4645–4653.
- (3) Arceo, E.; Marsden, P.; Bergman, R. G.; Ellman, J. A. *Chem. Commun.* **2009**, 3357–3359.
- (4) Schlaf, M.; Ghosh, P.; Fagan, P. J.; Hauptman, E.; Bullock, R. M. *Adv. Synth. Catal.* **2009**, *351*, 789–800.
- (5) Zakzeski, J.; Bruijninx, P. C. A.; Jongerius, A. L.; Weckhuysen, B. M. *Chem. Rev.* **2010**, *110*, 3552–3599.
- (6) Xu, X.; Li, Y.; Gong, Y.; Zhang, P.; Li, H.; Wang, Y. *J. Am. Chem. Soc.* **2012**, *134*, 16987–16990.
- (7) Nichols, J. M.; Bishop, L. M.; Bergman, R. G.; Ellman, J. A. *J. Am. Chem. Soc.* **2010**, *132*, 12554–12555.
- (8) Sergeev, A. G.; Webb, J. D.; Hartwig, J. F. *J. Am. Chem. Soc.* **2012**, *134*, 20226–20229.
- (9) He, J.; Zhao, C.; Lercher, J. A. *J. Am. Chem. Soc.* **2012**, *134*, 20768–20775.
- (10) Hanson, S. K.; Wu, R.; Silks, L. A. P. *Angew. Chem., Intl. Ed.* **2012**, *51*, 3410–3413.
- (11) Wenkert, E.; Michelotti, E. L.; Swindell, C. S. *J. Am. Chem. Soc.* **1979**, *101*, 2246–2247.
- (12) Wenkert, E.; Michelotti, E. L.; Swindell, C. S.; Tingoli, M. *J. Org. Chem.* **1984**, *49*, 4894–4899.
- (13) Dankwardt, J. W. *Angew. Chem., Intl. Ed.* **2004**, *43*, 2428–2432.

(14) Kakiuchi, F.; Usui, M.; Ueno, S.; Chatani, N.; Murai, S. *J. Am. Chem. Soc.* **2004**, *126*, 2706–2707.

(15) Ueno, S.; Mizushima, E.; Chatani, N.; Kakiuchi, F. *J. Am. Chem. Soc.* **2006**, *128*, 16516–16517.

(16) Guan, B.-T.; Xiang, S.-K.; Wang, B.-Q.; Sun, Z.-P.; Wang, Y.; Zhao, K.-Q.; Shi, Z.-J. *J. Am. Chem. Soc.* **2008**, *130*, 3268–3269.

(17) Guan, B.-T.; Xiang, S.-K.; Wu, T.; Sun, Z.-P.; Wang, B.-Q.; Zhao, K.-Q.; Shi, Z.-J. *Chem. Commun.* **2008**, 1437–1439.

(18) Tobisu, M.; Shimasaki, T.; Chatani, N. *Chem. Lett.* **2009**, *38*, 710–711.

(19) Shimasaki, T.; Konno, Y.; Tobisu, M.; Chatani, N. *Org. Lett.* **2009**, *11*, 4890–4892.

(20) Yu, D.-G.; Li, B.-J.; Shi, Z.-J. *Acc. Chem. Res.* **2010**, *43*, 1486–1495.

(21) Alvarez-Bercedo, P.; Martin, R. *J. Am. Chem. Soc.* **2010**, *132*, 17352–17353.

(22) Sergeev, A. G.; Hartwig, J. F. *Science* **2011**, *332*, 439–443.

(23) Tobisu, M.; Yamakawa, K.; Shimasaki, T.; Chatani, N. *Chem. Commun.* **2011**, *47*, 2946–2948.

(24) Guan, B.-T.; Wang, Y.; Li, B.-J.; Yu, D.-G.; Shi, Z.-J. *J. Am. Chem. Soc.* **2008**, *130*, 14468–14470.

(25) Li, B.-J.; Li, Y.-Z.; Lu, X.-Y.; Liu, J.; Guan, B.-T.; Shi, Z.-J. *Angew. Chem., Intl. Ed.* **2008**, *47*, 10124–10127.

(26) Quasdorf, K. W.; Tian, X.; Garg, N. K. *J. Am. Chem. Soc.* **2008**, *130*, 14422–14423.

(27) Li, Z.; Zhang, S.-L.; Fu, Y.; Guo, Q.-X.; Liu, L. *J. Am. Chem. Soc.* **2009**, *131*, 8815–8823.

(28) Li, B.-J.; Li, Y.-Z.; Lu, X.-Y.; Liu, J.; Guan, B.-T.; Shi, Z.-J. *Angew. Chem., Intl. Ed.* **2009**, *48*, 1351.

(29) Li, B.-J.; Xu, L.; Wu, Z.-H.; Guan, B.-T.; Sun, C.-L.; Wang, B.-Q.; Shi, Z.-J. *J. Am. Chem. Soc.* **2009**, *131*, 14656–14657.

(30) Shimasaki, T.; Tobisu, M.; Chatani, N. *Angew. Chem., Intl. Ed.* **2010**, *49*, 2929–2932.

(31) Huang, K.; Yu, D.-G.; Zheng, S.-F.; Wu, Z.-H.; Shi, Z.-J. *Chem.—Eur. J.* **2011**, *17*, 786–791.

(32) Manbeck, K. A.; Kundu, S.; Walsh, A. P.; Brennessel, W. W.; Jones, W. D. *Organometallics* **2012**, *31*, 5018–5024.

(33) Lu, Z.; Ma, S. *Angew. Chem., Intl. Ed.* **2008**, *47*, 258–297.

(34) Trost, B. M.; Van, V. D. L. *Chem. Rev.* **1996**, *96*, 395–422.

(35) Trost, B. M.; Crawley, M. L. *Chem. Rev.* **2003**, *103*, 2921–2943.

(36) Fang, P.; Raj Chaulagain, M.; Aron, Z. D. *Org. Lett.* **2012**, *14*, 2130–2133.

(37) Barrios-Landeros, F.; Hartwig, J. F. *J. Am. Chem. Soc.* **2005**, *127*, 6944–6945.

(38) Some reviews of alkane C–H bond activation by organometallic complexes: (a) Jones, W. D. *Science* **2000**, *287*, 1942–1943.

(b) Labinger, J. A.; Bercaw, J. E. *Nature* **2002**, *417*, 507–514.

(c) Goldberg, K. I.; Goldman, A. S., Eds. *Activation and Functionalization of C–H Bonds*; ACS Symposium Series 885; American Chemical Society: Washington, DC, 2004. [http://rutchem.rutgers.edu/~agoldman/TOC\\_ACS\\_Symposium\\_Series\\_885.htm](http://rutchem.rutgers.edu/~agoldman/TOC_ACS_Symposium_Series_885.htm)

(d) Crabtree, R. H. *Chem. Rev.* **2010**, *110*, 575. (e) Balcells, D.; Clot, E.; Eisenstein, O. *Chem. Rev.* **2010**, *110*, 749–823.

(39) Hartwig, J. F. In *Organotransition Metal Chemistry*; University Science Books: Sausalito, CA, 2010, pp 261–320.

(40) Crabtree, R. H. In *The Organometallic Chemistry of the Transition Metals*, 4th ed.; John Wiley & Sons: New York, 2005, pp 159–182 and 364–370.

(41) Ittel, S. D.; Tolman, C. A.; English, A. D.; Jesson, J. P. *J. Am. Chem. Soc.* **1978**, *100*, 7577–7585.

(42) Tolman, C. A.; Ittel, S. D.; English, A. D.; Jesson, J. P. *J. Am. Chem. Soc.* **1979**, *101*, 1742–1751.

(43) Zhu, Y.; Smith, D. A.; Herbert, D. E.; Gatard, S.; Ozerov, O. V. *Chem. Commun.* **2012**, *48*, 218–220.

(44) Bonanno, J. B.; Henry, T. P.; Neithamer, D. R.; Wolczanski, P. T.; Lobkovsky, E. B. *J. Am. Chem. Soc.* **1996**, *118*, 5132–5133.

(45) van der Boom, M. E.; Liou, S.-Y.; Ben-David, Y.; Vigalok, A.; Milstein, D. *Angew. Chem., Intl. Ed. Engl.* **1997**, *36*, 625–626.

- (46) van der Boom, M. E.; Liou, S.-Y.; Ben-David, Y.; Shimon, L. J. W.; Milstein, D. *J. Am. Chem. Soc.* **1998**, *120*, 6531–6541.
- (47) Trovitch, R. J.; Lobkovsky, E.; Bouwkamp, M. W.; Chirik, P. J. *Organometallics* **2008**, *27*, 6264–6278.
- (48) Komiya, S.; Suzuki, J.; Miki, K.; Kasai, N. *Chem. Lett.* **1987**, 1287–90.
- (49) For an unusual example of reductive elimination of C(sp<sup>3</sup>)–O bonds from a palladium center, see: Marquard, S. L.; Hartwig, J. F. *Angew. Chem., Intl. Ed.* **2011**, *50*, 7119–7123.
- (50) (a) Lara, P.; Paneque, M.; Poveda, M. L.; Salazar, V.; Santos, L. L.; Carmona, E. *J. Am. Chem. Soc.* **2006**, *128*, 3512–3513. (b) Conejero, S.; Paneque, M.; Poveda, M. L.; Santos, L. L.; Carmona, E. *Acc. Chem. Res.* **2010**, *43*, 572–580. (c) Santos, L. L.; Mereiter, K.; Paneque, M. *Organometallics* **2013**, *32*, 565–569.
- (51) Whited, M. T.; Grubbs, R. H. *Acc. Chem. Res.* **2009**, *42*, 1607–1616.
- (52) Whited, M. T.; Zhu, Y.; Timpa, S. D.; Chen, C.-H.; Foxman, B. M.; Ozerov, O. V.; Grubbs, R. H. *Organometallics* **2009**, *28*, 4560–4570.
- (53) Gupta, M.; Hagen, C.; Flesher, R. J.; Kaska, W. C.; Jensen, C. M. *Chem. Commun.* **1996**, 2083–2084.
- (54) Xu, W.; Rosini, G. P.; Gupta, M.; Jensen, C. M.; Kaska, W. C.; Krogh-Jespersen, K.; Goldman, A. S. *Chem. Commun.* **1997**, 2273–2274.
- (55) Liu, F.; Pak, E. B.; Singh, B.; Jensen, C. M.; Goldman, A. S. *J. Am. Chem. Soc.* **1999**, *121*, 4086–4087.
- (56) Kanzelberger, M.; Singh, B.; Czerw, M.; Krogh-Jespersen, K.; Goldman, A. S. *J. Am. Chem. Soc.* **2000**, *122*, 11017–11018.
- (57) Ghosh, R.; Emge, T. J.; Krogh-Jespersen, K.; Goldman, A. S. *J. Am. Chem. Soc.* **2008**, *130*, 11317–11327.
- (58) Morales-Morales, D.; Lee, D. W.; Wang, Z.; Jensen, C. M. *Organometallics* **2001**, *20*, 1144–1147.
- (59) Morales-Morales, D.; Redon, R.; Wang, Z.; Lee, D. W.; Yung, C.; Magnuson, K.; Jensen, C. M. *Can. J. Chem.* **2001**, *79*, 823–829.
- (60) Kanzelberger, M.; Zhang, X.; Emge, T. J.; Goldman, A. S.; Zhao, J.; Incarvito, C.; Hartwig, J. F. *J. Am. Chem. Soc.* **2003**, *125*, 13644–13645.
- (61) Choi, J.; Wang, D. Y.; Kundu, S.; Choliy, Y.; Emge, T. J.; Krogh-Jespersen, K.; Goldman, A. S. *Science* **2011**, *332*, 1545–1548.
- (62) Some lead references and examples of C–O bond formation via reductive elimination: (a) Han, R.; Hillhouse, G. L. *J. Am. Chem. Soc.* **1997**, *119*, 8135–8136. (b) Widenhofer, R. A.; Buchwald, S. L. *J. Am. Chem. Soc.* **1998**, *120*, 6504–6511. (c) Dick, A. R.; Kampf, J. W.; Sanford, M. S. *J. Am. Chem. Soc.* **2005**, *127*, 12790–12791. (d) Hartwig, J. F. *Synlett* **2006**, 1283–1294. (e) Vedernikov, A. N.; Binfield, S. A.; Zavalij, P. Y.; Khusnutdinova, J. R. *J. Am. Chem. Soc.* **2006**, *128*, 82–83. (f) Khusnutdinova, J. R.; Zavalij, P. Y.; Vedernikov, A. N. *Organometallics* **2007**, *26*, 3466–3483. (g) Hartwig, J. F. *Nature* **2008**, *455*, 314–322. (h) Racowski, J. M.; Dick, A. R.; Sanford, M. S. *J. Am. Chem. Soc.* **2009**, *131*, 10974–10983. (i) Vedernikov, A. N. *Top. Organomet. Chem.* **2010**, *31*, 101–121.
- (63) (a) Williams, B. S.; Holland, A. W.; Goldberg, K. I. *J. Am. Chem. Soc.* **1999**, *121*, 252–253. (b) Williams, B. S.; Goldberg, K. I. *J. Am. Chem. Soc.* **2001**, *123*, 2576–2587.
- (64) Choi, J.; Choliy, Y.; Zhang, X.; Emge, T. J.; Krogh-Jespersen, K.; Goldman, A. S. *J. Am. Chem. Soc.* **2009**, *131*, 15627–15629.
- (65) Renkema, K. B.; Kissin, Y. V.; Goldman, A. S. *J. Am. Chem. Soc.* **2003**, *125*, 7770–7771.
- (66) Ghosh, R.; Zhang, X.; Achord, P.; Emge, T. J.; Krogh-Jespersen, K.; Goldman, A. S. *J. Am. Chem. Soc.* **2007**, *129*, 853–866.
- (67) Slugovc, C.; Mereiter, K.; Trofimenko, S.; Carmona, E. *Angew. Chem., Intl. Ed.* **2000**, *39*, 2158–2160.
- (68) Jones, R. A.; Wilkinson, G. J. *Chem. Soc., Dalton Trans.* **1979**, 472–477.
- (69) Santos, L. L.; Mereiter, K.; Paneque, M.; Slugovc, C.; Carmona, E. *New J. Chem.* **2003**, *27*, 107–113.
- (70) Lara, P.; Paneque, M.; Poveda, M. L.; Santos, L. L.; Valpuesta, J. E. V.; Carmona, E.; Moncho, S.; Ujaque, G.; Lledós, A.; Álvarez, E.; Mereiter, K. *Chem.—Eur. J.* **2009**, *15*, 9034–9045.
- (71) Carbo, J. J.; Eisenstein, O.; Higgitt, C. L.; Klahn, A. H.; Maseras, F.; Oelckers, B.; Perutz, R. N. *J. Chem. Soc., Dalton Trans.* **2001**, 1452–1461.
- (72) Evans, M. E.; Burke, C. L.; Yaibuathes, S.; Clot, E.; Eisenstein, O.; Jones, W. D. *J. Am. Chem. Soc.* **2009**, *131*, 13464–13473.
- (73) Tanabe, T.; Brennessel, W. W.; Clot, E.; Eisenstein, O.; Jones, W. D. *Dalton Trans.* **2010**, *39*, 10495–10509.
- (74) Clot, E.; Besora, M.; Maseras, F.; Megret, C.; Eisenstein, O.; Oelckers, B.; Perutz, R. N. *Chem. Commun.* **2003**, 490–491.
- (75) Clot, E.; Megret, C.; Eisenstein, O.; Perutz, R. N. *J. Am. Chem. Soc.* **2009**, *131*, 7817–7827.
- (76) In this case, the product-determining step is presumably also the rate-determining step (vide infra). However, if, for example, elimination of TBE is rate-determining, the competition experiment would be equally informative regarding the subject of interest, i.e., mechanism of the reaction of (PCP)Ir with ether; the observed KIE would be the same as in the (presumably actual) case of reversible TBE loss prior to reaction of (PCP)Ir with ether.
- (77) Villano, S. M.; Kato, S.; Bierbaum, V. M. *J. Am. Chem. Soc.* **2006**, *128*, 736–737.
- (78) Yamataka, H.; Ando, T. *J. Phys. Chem.* **1981**, *85*, 2281–2286.
- (79) On the basis of calculations using PBE functionals, as opposed to the M06 functionals used in this work, we previously (ref 64) calculated a larger energy difference in favor of OAr migration, leading us to suggest that H-to-methylidene migration was the rate-determining step. We were, however, unable to easily reconcile the observed KIE (4.3) with the KIE thus calculated (7.2). In view of this dependence found on the particular functionals employed, and at the suggestion of an anonymous reviewer, we have also investigated the use of a range of other commonly applied functionals (M06-L, M06-2X, PBE, TPSS, TPSSH, B3LYP) to calculate the energies of the two key TS's (the TS's for  $\alpha$ -aryloxy elimination and for Ir-to-methylene hydride migration) and the predicted KIEs. With all functionals used, the two TSs are calculated to be fairly close in energy (within 4 kcal/mol of each other). The use of M06-2X leads to the prediction, in agreement with our conclusion, that the  $\alpha$ -aryloxy elimination TS is higher in energy (albeit by only 1.1 kcal/mol) than the TS for Ir-to-methylene hydride migration. Full results of these calculations are given in Table S6 of the Supporting Information.
- (80) We find it useful to express the overall KIE in terms of the relative rates of the reaction of isotopomeric ethers with free (PCP)Ir although free (PCP)Ir is clearly not the resting state for this system. This yields, for each isotopomer,  $k_X = K_{SX}[(PCP)Ir] \bullet k_{9X}$ . The key condition on which this analysis is based is that (PCP)Ir(CH<sub>2</sub>OAr) (H) and (PCP)Ir(CD<sub>2</sub>OAr) (D) are in equilibrium with each other. This must be the case if the rate-determining step is subsequent to the formation of these species on the reaction pathway. We express this in terms of an equilibrium with (PCP)Ir, although it could be expressed as an equilibrium with any other species (resting state, intermediate, or even a purely hypothetical species); the free energy of that species will be canceled out of the final equation. In this case, specifically, the free energy difference of (PCP)Ir(CH<sub>2</sub>OAr) (H) (plus free CD<sub>3</sub>OAr) vs (PCP)Ir(CD<sub>2</sub>OAr) (D) (plus free CH<sub>3</sub>OAr) is equal to  $-\Delta\Delta G_8$  kcal/mol; which is necessarily equal to  $\Delta\Delta G_8$  where  $EIE_8 = \exp(-\Delta\Delta G_8/RT)$ .
- (81) See, for example: (a) Parkin, G. *Acc. Chem. Res.* **2009**, *42*, 315–325. (b) Janak, K. E.; Parkin, G. *J. Am. Chem. Soc.* **2003**, *125*, 6889–6891 and references therein.
- (82) (a) Rachidi, I. E.-I.; Eisenstein, O.; Jean, Y. *New J. Chem.* **1990**, *14*, 671–677. (b) Riehl, J.-F.; Jean, Y.; Eisenstein, O.; Pélissier, M. *Organometallics* **1992**, *11*, 729.
- (83) Chan, J.; Tang, A.; Bennet, A. J. *J. Am. Chem. Soc.* **2012**, *134*, 1212–1220.
- (84) Singh, V.; Schramm, V. L. *J. Am. Chem. Soc.* **2007**, *129*, 2783–2795.
- (85) Adcock, W.; Trout, N. A.; Vercoe, D.; Taylor, D. K.; Shiner, V. J.; Sorensen, T. S. *J. Org. Chem.* **2003**, *68*, 5399–5402.
- (86) Asperger, S.; Kukric, Z.; Saunders, W. H.; Sutic, D. *J. Chem. Soc., Perkin Trans. 2* **1992**, 275–279.



- (87) Asperger, S.; Pavlovic, D.; Kukric, Z.; Sutic, D. *Inorg. Chim. Acta* **1990**, *171*, 5–9.
- (88) Sutic, D.; Asperger, S.; Borcic, S. *J. Org. Chem.* **1982**, *47*, 5120–4.
- (89) Streitwieser, A.; Dafforn, G. A. *Tetrahedron Lett.* **1969**, *10*, 1263–1266.
- (90) Shiner, V. J.; Rapp, M. W.; Halevi, E. A.; Wolfsberg, M. *J. Am. Chem. Soc.* **1968**, *90*, 7171–7172.
- (91) Kundu, S.; Choi, J.; Krogh-Jespersen, K.; Emge, T. J.; Goldman, A. S. *Abstracts of Papers, 237th ACS National Meeting, Salt Lake City, UT, United States, March 22–26, 2009*, INOR-668.
- (92) Previous reports of bond cleavage analogous to the carboalkoxy C–O bond were limited to allyl and vinyl esters: (a) Yamamoto, A. *Adv. Organomet. Chem.* **1992**, *34*, 111. (b) Tatsumi, T.; Tominaga, H.; Hidai, M.; Uchida, Y. *J. Organomet. Chem.* **1981**, *218*, 177.
- (93) Examples of acyl C–O bond cleavage in esters: (a) Tatamidani, H.; Yokota, K.; Kakiuchi, F.; Chatani, N. *J. Org. Chem.* **2004**, *69*, 5615. (b) Yamamoto, Y.; Han, X.-H.; Ma, J.-F. *Angew. Chem., Int. Ed.* **2000**, *39*, 1965. (c) Hiraki, K.; Kira, S.-i.; Kawano, H. *Bull. Chem. Soc. Jpn.* **1997**, *70*, 1583. (d) Grotjahn, D. B.; Joubbran, C. *Organometallics* **1995**, *14*, 5171. (e) Yamamoto, T.; Miyashita, S.; Naito, Y.; Komiya, S.; Ito, T.; Yamamoto, A. *Organometallics* **1982**, *1*, 808. (f) Yamamoto, T.; Ishizu, J.; Kohara, T.; Komiya, S.; Yamamoto, A. *J. Am. Chem. Soc.* **1980**, *102*, 3758.
- (94) Zhang, X.; Kanzelberger, M.; Emge, T. J.; Goldman, A. S. *J. Am. Chem. Soc.* **2004**, *126*, 13192–13193.
- (95) Rybtchinski, B.; Vigalok, A.; Ben-David, Y.; Milstein, D. *J. Am. Chem. Soc.* **1996**, *118*, 12406–12415.
- (96) For examples of the (PCP–CH<sub>2</sub>) ligand motifs in Rh and Ni complexes, see: (a) Vigalok, A.; Rybtchinski, B.; Shimon, L. J. W.; Ben-David, Y.; Milstein, D. *Organometallics* **1999**, *18*, 895. (b) van der Boom, M. E.; Liou, S.-Y.; Shimon, L. J. W.; Ben-David, Y.; Milstein, D. *Inorg. Chim. Acta* **2004**, *357*, 4015.
- (97) Romero, P. E.; Whited, M. T.; Grubbs, R. H. *Organometallics* **2008**, *27*, 3422–3429.
- (98) Whited, M. T.; Grubbs, R. H. *J. Am. Chem. Soc.* **2008**, *130*, 5874–5875.
- (99) Zhang, X.; Wang, D. Y.; Emge, T. J.; Goldman, A. S. *Inorg. Chim. Acta* **2011**, *369*, 253–259.
- (100) See Supporting Information.
- (101) Bradley, C. A.; Veiros, L. F.; Pun, D.; Lobkovsky, E.; Keresztes, I.; Chirik, P. J. *J. Am. Chem. Soc.* **2006**, *128*, 16600–16612.
- (102) Bradley, C. A.; Veiros, L. F.; Chirik, P. J. *Organometallics* **2007**, *26*, 3191–3200.
- (103) Williams, B. S.; Leatherman, M. D.; White, P. S.; Brookhart, M. *J. Am. Chem. Soc.* **2005**, *127*, 5132–5146.
- (104) Zhao, Y.; Truhlar, D. G. *Theor. Chem. Acc.* **2008**, *120*, 215–241.
- (105) (a) Hay, P. J. W.; Wadt, W. R. *J. Chem. Phys.* **1985**, *82*, 299. (b) Roy, L. E.; Hay, P. J.; Martin, R. L. *J. Chem. Theory Comput.* **2008**, *4*, 1029.
- (106) (a) Woon, D. E.; Dunning, T. H., Jr. *J. Chem. Phys.* **1993**, *98*, 1358. (b) Dunning, T. H., Jr. *J. Chem. Phys.* **1989**, *90*, 1007. (c) Kendall, R. A.; Dunning, T. H., Jr.; Harrison, J. R. *J. Chem. Phys.* **1992**, *96*, 6796.